To
The Associate Editor

Sub: Submission of manuscript “Quantification of multiple simultaneously occurring nitrogen flows in the euphotic ocean” for publication in *Biogeosciences*.

Dear Prof. Middelburg,

Thank you for your assistance on the process of our manuscript.

To more clearly present the capability of our method, we reorganized the manuscript and enhanced the discussion. We followed reviewer’s suggestions introducing the simple (low nutrient) first and then the complex case (high nutrient). Such sequence remains throughout the manuscript.

We modified the model slightly to explore more processes associated with NH_4^+, including remineralization and ammonium uptake by bacteria, both were previously found important in incubation experiments. However, NO_2^- release from PON pool was removed by assuming nitrate reduction is minor among N processes. Since nitrate reduction is an intra cellular process, we also assume nitrite release would follow the r value of nitrate pool not influencing the isotopic composition of NO_x^- (nitrite and nitrate were pulled into one compartment, NO_x^-, in the low nutrient case), thus, the determination of other NO_x^- pool associated processes. Nitrite release was removed due to similar reasons for the high nutrient case. After removing one and adding two unknowns, both low and high nutrient cases can be expressed by matrix equations with unique solutions according to ^{14}N and ^{15}N mass balances of system level.

Many questions were raised by reviewers due to our under-description and mathematical notation regarding equations and derivation. All the equations were re-written by replacing dC/dt with $\Delta C/\Delta t$. We clarify all points raised and introduced details about rate derivations. We applied the first two points to calculate process rates, differing from that via ordinary differential equation (ODE, time course required). Although unique solution can be obtained, we still applied ODE for comparison (results in new tables). We did sensitivity test for the unique solution, however, the

results were shown in the reply not in the updated main text to avoid distractions. According to Reviewer#3's comments, we also added one more experimental case of low light water (2% sPAR) to reveal more ecological implications. More discussions in comparisons with previous models in terms of model structure and rate numbers were added into Discussion. The time course projection provided by STELLA was termed as validation rather than back calculation since we predict the temporal variation for 24 hours by using the rate numbers derived from the first two time points. More biogeochemical implications, such as remineralization and phytoplankton community succession, the contribution of nitrification to new production, nutrient preference and the ammonium consumption pathways, were made separately in the Section 2 of Discussion.

According to additional descriptions and discussions, the total length of this version was similar to that of the old version. However, the scientific level of this paper was promoted due to constructive comments from reviewers. We believe the current version is qualified for publication in Biogeosciences.

Yours sincerely,

Shuh-Ji Kao

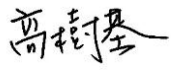

December 9, 2016

Referee #1, comment #1

The authors present a ms that utilizes sets of linear equations (as a matrix model) to describe nitrogen transformations in seawater from 25 meter depth. The authors argue that 'conventional methods' for calculating rates, including nitrification, do not consider that multiple nitrogen processes are occurring simultaneously. The authors present the model, and then illustrate 2 manipulations where enriched $^{15}NH_4^+$ was added to determine what nitrogen pools it ends up in. They use the program STELLA to estimate parameters of their model. They conclude that NH_4^+ regeneration is likely an important process through isotope dilution, that their model can give differing results from the 'traditional model', and that DON is likely very important. They were able to solve for multiply occurring processes. This is an interesting ms and the community will be interested in the approach. The authors, however, need to address a number of comments to make this a more significant ms.

Author response:

Thanks for reviewer's appreciation of the merit of our method.

Referee #1, comment #2

The recognition that there are multiple nitrogen transformations is an important one, and the coupling of the model to an enrichment assay is a strong approach. Although I appreciate what the authors are doing here, the statement that they are the first to do needs to be amended, given the recent publication of Pfister et al. in BGS. Biogeosciences, 13, 3519-3531, 2016, http://www.biogeosciences.net/13/3519/2016/ ("To our knowledge, this is the first and most convenient method designed to quantitatively and simultaneously resolve complicated nitrogen transformation rates, albeit with some uncertainties."). Thus, throughout the discussion it would be appropriate to see their model compared with the differential equation model used by Pfister et al. to model multiple nitrogen transformations. The authors also need to compare their conclusions with the above study. For example, I note that this study follows processes in seawater only, while Pfister et al. includes benthic species. It would be useful for the authors to comment on the comparisons.

Author response:

This is a very constructive suggestion. Indeed, we missed the paper by Pfister et al. (2016) while we submitted our manuscript in July. Pfister et al. (2016) applied similar approach to resolve the N cycle processes in a tidal pool. In this version, we introduced the paper by Pfister et al. (2016) in Introduction. As suggested also by Reviewer #2, we made discussions and comparisons with their method for tidal pool.

The similarity is the coupled monitoring of changes in isotopic composition and concentration in multiple pools (NH_4^+, NO_2^- and NO_3^-). However, dissimilarities include：(1) we focused on water column and all operationally defined nitrogen pools were measured, (2) the benthic biomass, which equals to particulate organic nitrogen

in our case, were not measured in their tidal pools; thus, system level mass conservation cannot be made. Accordingly, their case did not allow discussions of DON release, which is an important process in water column; (3) they applied ODE to derive the mean rate constant by fitting parameter combination over the monitoring time course; by contrast, we use matrix (or linear programming in old version) to obtain rate/rate constant for the first two data points and then predict latter on changes.

We thoroughly revised our manuscript basing on three reviewers' comments. In this version, we modified our model structure slightly (see the reply for Reviewer #2) and discussed more in term of model structure and method for rate derivation. The rates derived by using ODE were also added into our tables for comparison. Meanwhile, we reorganized the manuscript in sequence from simple (low nutrient assay) to complex case (high nutrient assay). We believe that such a re-arrangement will be easier for readers to understand our method.

We attempt to resolve rates in water column, more specifically, in sun-lit ocean where intensive substrate competition occurs, thus, we modified our original statement to "This is a convenient method in euphotic zone to quantitatively and simultaneously resolve complicated nitrogen transformation rates, albeit with some uncertainties.".

Referee #1, comment #3

The ms would benefit from more direct discussion about the comparison of the models presented in this paper and other models and approaches. Nitrogen processing rates don't seem to differ much based on methodology (Table 3), with values at least being within a similar range. I find this surprising, especially given the authors' recognition of error sources (L576). The abstract states: "comparisons with conventional labeling methods are discussed" (L28) and this is too vague. Similarly, the Conclusions could be stronger and more direct.

Author response:

The significance of our method is to resolve multiple rates by adding one single tracer in one bottle for incubation. This cannot be achieved by conventional methods. As mentioned above, Pfister et al. (2016) did not include DON in their discussion according to under-identified benthic biomass.

We highlighted the significance of our method; however, we do not criticize traditional methods. For example, the traditional method for nitrification was usually conducted in the dark or deep water, thus, the consumption of substrate (ammonium) and product (nitrate) by phytoplankton was minimized presumably. In the dark, the traditional approach is ok; however, bias could be significant in the euphotic zone where phytoplankton competition appears. Meanwhile, similar rate values (less biased) can be obtained by traditional methods when one or two specific processes dominate the system.

As mentioned in Elskens et al. (2005), none model was perfect. For example, in a simple system without phytoplankton and light there will be no need to apply our approach. As mentioned in manuscript already, the traditional estimate for nitrification does not work under simulated *in situ* light in the euphotic zone since the end-product, nitrate, drops quickly due to intensive phytoplankton consumption. Such drop in end-product violates the assumption "end-product increase" in traditional method. Thus, dark incubation is required to limit phytoplankton uptake. The incubation in the dark, of course, does not represent "*in situ*" condition. The advantages of our method are (1) to explore the transformation of pathways for *in situ* condition, particularly, in euphotic ocean and at around the transition zones (e.g., nitracline and thermocline in the field) and (2) to examine responses of multiple metabolic pathways via manipulation experiments (e.g., pH, temperature and light).

Finally, the rate numbers for ammonium, nitrate uptakes and nitrification in Table 3 revealed difference. Ours values are 3-20% higher than those by traditional methods. Moreover, nitrate uptake rate by our method was ~6 times higher (in Table 3) than that derived from the equation suggested by Santoro et al. (2010) although nitrification rate was within a similar range. In this version, we pointed out explicitly the reasons for the offset between ours and conventional methods. We enhanced comparisons among methods in Discussion part and made a stronger statement in Conclusions. We found the sentence "comparisons with conventional labeling methods are discussed" to be improper in the Abstract. We eliminated this sentence.

Referee #1, comment #4

The ms would benefit from adhering more strongly to a clear separation of methods, results, discussion. The paragraph starting L395 is a good example where this needs to be done. It might help to shorten the ms too.

Author response:

Follow this suggestion, the manuscript was reorganized. Examples were given together now in Methods from the simple to the complex case. Details for matrix solution and sensitivity test were now mentioned in Methods first and then appeared in Results. Yet, the entire length was expanded due to additional data presentation (we added 2% light incubation for comparison as requested), methodology comparison (we added results from ODE as requested; see reply to reviewer #2) and in-depth discussions.

Referee #1, comment #5

Finally, although I greatly appreciate the enrichment assay, it appears to be done once. I cannot be sure based on the description given, but it appears unreplicated and that does limit the interpretation the authors can make. Starting L314, more detail is needed including how many incubations, and whether they were replicates or uniquely treated. Having the high and low nutrient assay immediately next to each other in the methods would also lend better comparison. As is, it is looks like these

assays are unreplicated and water was collected at different depths, etc.

Author response:

We do have replicates. We added descriptions for replicates in this version. In the old version, two data points were representative of replicates. We now used regular and inverse triangles, which give a clearer image of data distribution (see panels below). Moreover, we provided a new case incubated under 2% light.

Instead of discussing the biogeochemical significance of specific processes, the scope of this paper is to propose a convenient method in the field for multiple rate measures. We agree with reviewer that replicates will be helpful indeed if we attempt to probe ecosystem biogeochemistry, however, not necessarily be helpful for a new method establishment. The rate uncertainty, in fact, was largely sourced from heterogeneity of water sample and analytical errors for isotopic composition and concentration, rather than the estimator itself.

The two assays, in fact, are for two very different yet commonly seen conditions. The simple one is for oligotrophic ocean (nitrite and nitrate were pulled together in one nitrogen pool, NO_x^-). The complex one is for estuary and coastal water where nitrite concentrations are relatively high. According to this suggestion, we illustrated both assays together in the Methods and reorganized the manuscript from the simple case to the complex case. To convince readers the applicability of our method, we presented additional data in this version to discuss these N transformation pathways under different light conditions (see panel (a) and (b) below). All the fluxes were derived from the matrix solution for the first two time points. The full time courses were generated via equation-based simulation by using Stella. We successfully and precisely predicted the observed time courses further illustrating the performance of our method.

(a) High nutrient case – 80% sPAR

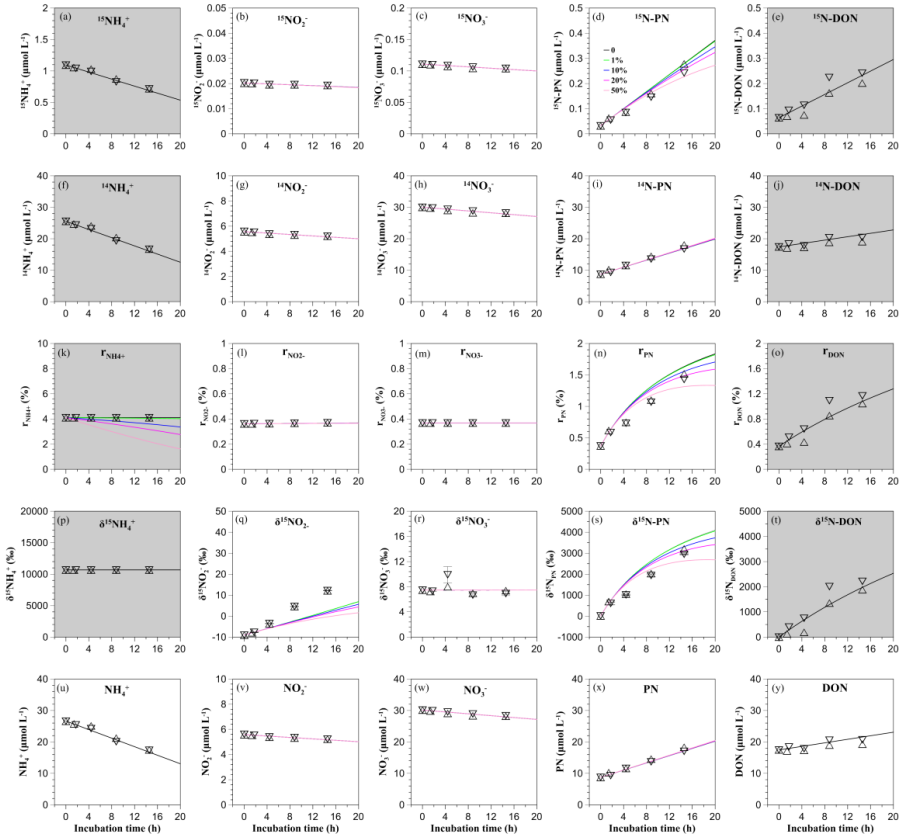

(b) High nutrient case – 2% sPAR

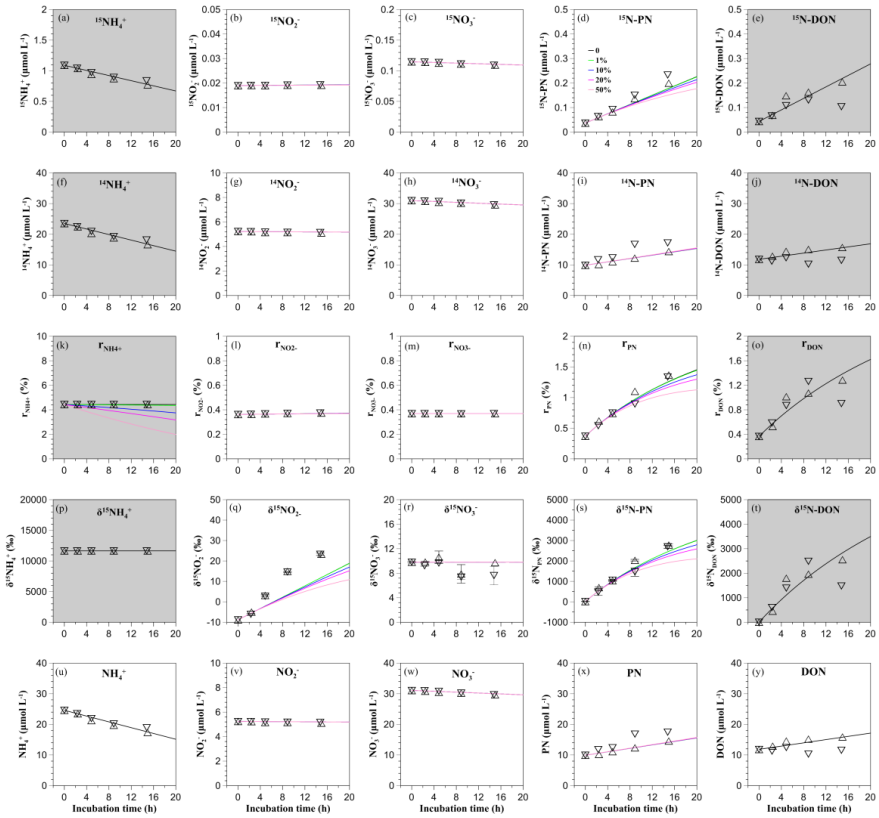

Referee #1, specific comments:

Line 50, explain what is meant by the ‘inventory method’

Author response:

We followed B. B. Ward (2011). The description is now “The inventory method (monitoring substrate and/or product changes over time) is often used …”.

Line 57“mainly”

Author response:

Corrected.

L105, 210 – be specific about what ‘new method’ means

Author response:

We changed to “isotope matrix” method.

L106, is STELLA a model or a method? What is meant by “The method was also validated using the STELLA model”.

Author response:

STELLA is user-friendly software for box model construction. We realized the appearance of Stella here in Introduction is improper, thus, this sentence was removed. The descriptions about STELLA will be in Methods.

L150, omit ‘basically’

Author response:

Omitted.

L210, what is the ‘incubation system’?

Author response:

We changed to incubation bottle.

L243,“approximately”

Author response:

Corrected.

L416, the depth of water collection for the experiment is unclear. Here it says 25 m, while elsewhere it states 3 m.

Author response:

We presented two samples collected from different locations. One was taken from the western North Pacific (low nutrient case) and the other was from a coastal bay in southern China (high nutrient case). In this version, we mentioned the two cases together in Methods to avoid confusion.

L419, the final enrichment value should be given.

Author response:

The description is now "…to achieve a final tracers concentration of 30 nM."

Methods – What were the dissolved oxygen levels? Is the assumption that this is a well-oxygenated system and loss of ^{15}N as gas is irrelevant?

Author response:

Yes. We made assumptions for oxygenated water column and short term incubation. Such assumption is common and well accepted. In this version, we provided DO saturation values for all cases.

L482 'result'

Author response:

Corrected.

Though I could read eqns 5, 6, 7, they are reprinted poorly due to some 'translation' issue.

Author response:

We tried several times and even asked editorial office's help for file translation during our initial submission. The problem was due to version of software. We will work it out.

L552 – Is there good evidence for light inhibition? Many studies find high rates of nitrification with normal light.

Author response:

Light depresses nitrification efficiency by either direct inhibition on AMO or resource reallocation for damage recovery. Similar to previous studies, such as Merbt et al. (2012), Smith et al. (2014) and Peng et al. (2016), we found light inhibition also in coastal China seas although some recent evidences showed that some taxa of marine AOA hold genetic capabilities to reduce oxidative stress and to repair ultraviolet damage (Luo et al., 2014; Santoro et al., 2015). In the photic ocean, besides photo damage nitrifiers need to compete with phytoplankton for substrate. This is why the abundance of AOA/B increased downward in genera and also why we establish this method to explore competing processes under in situ light condition.

According to this question and reviewer #3's suggestion, we presented additional data for the high nutrient case. For high nutrient case, actually, water from 80% sPAR and 2% sPAR were sampled for incubation. We measured fluxes for multiple pathways for different light environments, and then discussed effects of light on nitrification.

The authors do not need to comment so much on inhibitors – which they did not use.

Author response:

We did not criticize the usefulness of inhibitor method since to block unwanted process is the only way to obtain a more accurate rate measure for specific process while using the traditional source-product method. Although inhibitor addition was not used in isotope labelling method, similar concept was applied to reduce the interference from unwanted pathway; such as nitrification rate measurement needs to be conducted in the dark to minimize ammonium and nitrate consumptions by phytoplankton. In this version, we removed the statement of inhibitor application.

Table 1 caption – explain "different r_{NH4+} variation". What seems to be meant here is that the authors are manipulating the values of r_{NH4+} to mimic the effects of isotope dilution as a consequence of regeneration.

Author response:

Yes, we did not measure isotopic compositions for NH_4^+. Thus, after obtaining fluxes (or rate constants) we set r_{NH4+} as variable to examine the significance of remineralization in short term incubation. Results showed that remineralization would be effective in our case when incubation is prolonged over 12 hours. According to the validation by consecutive observations, remineralization is limited in all our cases in the first few hours. We added more discussions about the sensitivity test for remineralization.

We mentioned in the manuscript that once the technique for isotopic composition of low concentration NH_4^+ is mature (open ocean case) or in any case r_{NH4+} time course was measured (coastal ocean case), all rates including remineralization can be

obtained directly. Here in our case, we simulated the time courses of different nitrogen pools and assessed the importance of regeneration by manipulating r_{NH4+}.

Same for Table 2 caption. Table 3 – Provide a citation for the Traditional Rate Calculation (Collos, 1987) and cite the equation numbers used for each.

Author response:

Reference was added.

Suppl. fig 1 and 2 are STELLA figs which can be confusing without equations. I did not get much out of these figs, other than the recognition that the authors used this model structure.

Author response:

We added equations into the two panels in this version.

Throughout the ms, the authors need to check that chemical terminology is reprinted accurately. Similarly, when subscripts are used.

Author response:

Thanks for reminding. We checked these terms carefully and will try our best to solve problems caused by format translation.

Dear Editor,

We found all comments are constructive. However, some questions regarding methods were raised due to our under-descriptions in old version. We also modified slightly the model structure for both low and high nutrient cases in order to examine the processes of remineralization, DON release and ammonium uptake by microbes (< 0.7 um). As replied below, our method was simply the integration of the first two time points (trapezoid method) and unique solution can be obtained. According to comments below, we applied ODE and present the ODE-derived results in tables for comparison. The differences in rate or rate constants were caused by length for time integration. However, we need to emphasize this paper is not a model paper. The constructed box model was based on our questions just to project these full time courses of oft-measured pools for validation. Addition to the model extrapolation, we ran sensitivity test for these rate numbers to convince readers the reliability of matrix-derived values. The manuscript had been reorganized and the part of methodology was thoroughly revised.

On behalf of all the authors

Sincerely,

Shuh Ji Kao

Reviewer #2, comment #1

Min Nina Xu and co-workers present an original experimental design to quantify multiple nitrogen transformation processes (rates of ammonium, nitrite and nitrate uptake, ammonia oxidation; nitrite oxidation; nitrite excretion; DON release; and potentially remineralization) by adding a single ^{15}N-labelled ammonium substrate into a single incubation system. No inhibitors were used and special attention was given to minimize the alteration of the system by adding a limited amount of tracer. Examples of field measurements are presented and different calculation methods are discussed. The article is written in a clear and understandable manner and fits well with the scope of Biogeosciences (BG). The study is worthy of publication but the authors need to address a number of comments to improve their manuscript (ms).

Author response:

Thanks.

Reviewer #2, comment #2

I have a concern about the method used to solve the rate law equations. Here the mass balance differential equations for determining the N-transformation rates are not integrated, neither analytically or numerically. This is rather unusual and in opposition with standard methods acclaimed for the treatment of chemical reaction kinetics. Such an approach, using rates instead of the generated profile of concentrations versus time, presents serious drawbacks, namely regarding the uncertainty on the estimated parameters (rates or rate constants). Unfortunately, this point is not addressed in the ms. The authors should therefore convince the reader that their method is at least as good as conventional integration methods in terms of accuracy and precision, and this requires an uncertainty assessment (see specific comments).

Author response:

To avoid confusion, we change dC/dt into $\Delta C/\Delta t$.

The rate constants were determined by using the measurements at time zero and the first time point after that. The matrix equations were not constructed for calculating derivatives but to integrate the differential equation between the first two time points, and then to estimate the "instant flux" (F or $k^* \bar{C}$, if time for incubation is short enough). Note that the use of "instant" here is just to make it distinguishable from the longer time incubation (or > two time points). The method we used was a second-order Runge-Kutta method, more specifically, the improved Euler method, to carry out the integration numerically. In our case, we inverted the solutions to solve for the fluxes or rate constants that would give us the correct answers at the first time point. Because the fluxes and rate constants are determined entirely from the data at time zero and the first time point, our method is equivalent to integrating the functions (trapezoid method).

After having the "instant rate" for the first time interval, we constructed a box model (equation-based input-output box model) to predict (i.e., extrapolation) the full time courses for all nitrogen pools. In previous version, the model structures and the numbers of equations and unknowns for the two cases were different (see below). However, we did not describe clearly in old version. More details will be given regarding the derivation procedure. The number of equation equals the number of unknown. Thus, no uncertainty exists for the matrix solution. However, reviewer is correct for the uncertainty induced by limited data points for derivation. The major uncertainty will be sourced from analytical uncertainties and sample heterogeneity. However, in all our cases, these extrapolations agreed well with consecutive observations, suggesting a good performance of our estimator for rate or rate constant with good measurements. In this version, we stated explicitly that researchers can applied our approach by using more observational data (enlarged trapezoid) to get an

average rate for longer duration if ignorable community change can be assured (see example blow for low nutrient case).
According to reviewers' comments, we modified the model slightly (see revised model structures below for comment #4) and described the two cases together in Methods.

Reviewer #2, comment #3

The authors are not the first to propose a mass balance approach to derive multiple N-transformation rates. As far as I know, such an approach was used and discussed at least in three previous publications. 1. Elskens et al., Global Biogeochemical Cycles, vol. 19, gb4028, doi:10.1029/2004gb002332, GBC-2005 2. De Brauwere et al. Chemometrics and Intelligent Laboratory Systems 76, 163– 173, CILS-2005 3. Pfister et al., Biogeosciences, 13, 3519–3531, BGS-2016. In the GBC approach, the rate law equations are analytically integrated while in the BGS, the differential equations are solved numerically using an ODE function. Currently the use of the ODE function for solving ordinary differential equations is easy to implement (see https://cran.rproject.org/web/packages/deSolve/deSolve.pdf) and the generated profile of concentrations versus time can be fitted using least squares methods (see GBC, CILS and BGS papers). It would be appropriate to address these points in the introduction, and throughout the discussion, the authors should argue why their simplified approach can be an asset when compared to the aforementioned papers.

Author response:

Following this comment, we changed our statement about "mass balance". The statement is now "This is a convenient method specifically for euphotic zone to quantitatively and simultaneously resolve complicated nitrogen transformation rates, albeit with some uncertainties.". Above mentioned models had been referred in revision.
The rate derived from ODE is a mean of integration over time that requires a concentration time course (three points at least) for iteration and integration, thereby differs from our "instant rate" determined by two time points as replied above. Although our method is simple mathematically, we do integration. We agree with reviewer that ODE may have advantages with the support of longer time course, however, our two-point matrix solution also gave good performance for extrapolation (see figures for comment #5 by Reviewer #1).
Nevertheless, we applied ODE and made a comparison for fixed r_{NH4+} condition (see the example below for high nutrient case with 80% sPAR). The rate values obtained by matrix and ODE were consistent. The difference in rate, if any, was caused by the duration for integration, i.e., shorter time (two points for the first ~2 hours) for ours

and longer time (5 points for ~15 hours) for ODE. Since time series monitoring in prolonged on-deck incubation is inconvenient and inappropriate due to rapid nutrient turnover and microbial community change. Thus, we select the first two time points for integration. The model was constructed to reduce the potential bias in traditional source-product method caused by ^{15}N flows among boxes. Our aim is to provide a less biased and convenient (in term of on-deck implementation and post-hoc data processing) measure for multiple transformation rates (more specifically, the "instant rate" researchers are eager to know). As indicated by Elskens et al. (2005), over complex models can misinterpret part of the random noise as relevant processes. These boxes, i.e. PN, nitrate, nitrite and ammonium, were the most often measured species and these exchanges we applied among pools were the most fundamental processes.

Table 2a. Results of high nutrient case under 80% PAR.

Rate ($k \times \bar{C}$) nmol L^{-1} h^{-1}	The percentage of r_{NH4+} decrease in 15 h					
	0		1%	10%	20%	50%
	ODE*	Isotope Matrix	Isotope Matrix	Isotope Matrix	Isotope Matrix	Isotope Matrix
NH_4^+ uptake (F1)	361	397	397	399	401	408
Remineralization (F2)	0	0	21	211	424	1043
NO_2^- uptake (F3)	28	29	29	29	29	29
NH_4^+ oxidation (F4)	1.1	0.4	0.4	0.4	0.4	0.4
NO_3^- uptake (F5)	189	149	149	149	149	149
NO_2^- oxidation (F6)	1.1	0	0	0	0	0
DON release (F7)	0	0	0	0	0	0
Bacteria uptake NH_4^+ (F8)	268	282	303	490	701	1314

*Ordinary Differential Equation

Reviewer #2, comment #4

Also I'm not convinced that adding a single ^{15}N-labelled ammonium tracer into the incubation system allows an accurate determination of the ammonium, nitrite and nitrate uptake rates. According to me the kinetic reactions corresponding to the matrix expressions (Eqns 16-17) with the labelling of a single ammonium substrate is underidentified. Under this condition, the ^{15}N-labelling of PN proceeds via the uptake of ammonium and/or via nitrification and the subsequent uptakes of nitrite and nitrate. These processes are thus not independent, and may result in a multimodal optimization problem, i.e., multiple solutions providing similar responses. The authors

should address this point, especially because little information is available in the ms regarding the method used to solve Eqns. (16-17).

Author response:

Reviewer is correct about the optimization problem. We did not make clear and correct descriptions in our old version. The problem no longer exists after our modification.

In previous version for the simple case (low nutrient open ocean, include NO_2^- into NO_x^- as one pool), we set nitrite release from the PN pool along with r_{PN} (F5 in panel (a) of Figure r1 below). We found this not reasonable since nitrite release occurs during intra-cell nitrate reduction. Meanwhile, this flux should be minor relative to other fluxes. In this version, we modified the model structure, of which the nitrite release was included as an internal cycle inside the NO_x^- pool, which can be precisely measured by bacteria method. On the other hand, the remineralization input of NH_4^+ (F2) was connected to the DON pool instead of PN to more realistically reflect the dilution effect. As mentioned in our manuscript, once the isotopic composition of ammonium at the end-point can be measured accurately, no assumption or sensitivity test for r_{NH4+} is needed. Currently, we manipulated r_{NH4+} values to examine the effect of remineralization. Via our extrapolation process, the effect of remineralization was evaluated.

According to other reviewer's suggestion, we discussed the missing nitrogen for both high and low nutrient cases (see the example of F5 and F6 in panel (b) of Figure r1 below for low nutrient case), which had been pointed out yet unresolved in previous study by Laws (1985). Here in this version, F5 in low nutrient case was the DON release from PN following the isotope ratio of PN and F6 was defined as ammonium uptake by microbes that passed through the GF/F filter (0.7 μm).

The modified model structure is shown below in (b) accompanied with the old one in (a) for comparison. According to this modification, unique solution can be obtained by matrix (6 unknowns and 6 independent equations).

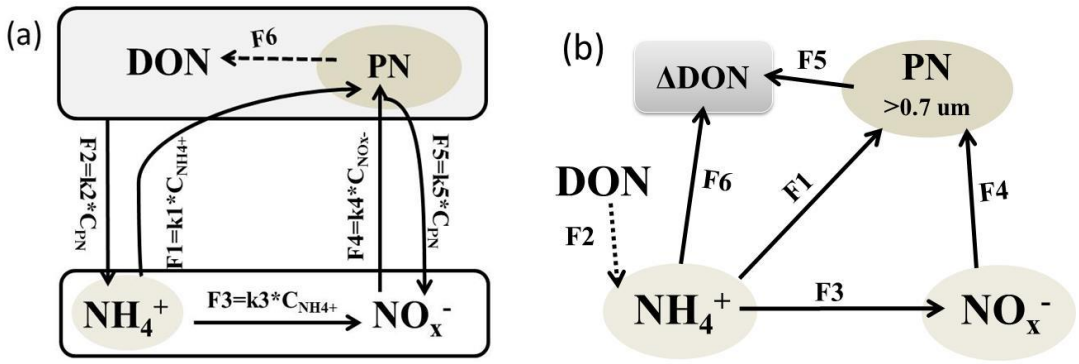

Figure r1. The old (a) and revised (b) model structures for low nutrient case.

Equations for the low nutrient case:

$$\frac{\Delta\left[{}^{15}NH_4^+\right]}{\Delta T} = \overline{F_2}\times 0.00366 - \overline{F_1}\times\overline{r_{NH_4^+}} - \overline{F_3}\times\overline{r_{NH_4^+}} - \overline{F_6}\times\overline{r_{NH_4^+}}$$

$$\frac{\Delta\left[{}^{15}NO_x^-\right]}{\Delta T} = \overline{F_3}\times\overline{r_{NH_4^+}} - \overline{F_4}\times\overline{r_{NO_x^-}}$$

$$\frac{\Delta\left[{}^{15}PN\right]}{\Delta T} = \overline{F_1}\times\overline{r_{NH_4^+}} + \overline{F_4}\times\overline{r_{NO_x^-}} - \overline{F_5}\times\overline{r_{PN}}$$

$$\frac{\Delta\left[{}^{14}NH_4^+\right]}{\Delta T} = \overline{F_2}\times(1-0.00366) - \overline{F_1}\times(1-\overline{r_{NH_4^+}}) - \overline{F_3}\times(1-\overline{r_{NH_4^+}}) - \overline{F_6}\times(1-\overline{r_{NH_4^+}})$$

$$\frac{\Delta\left[{}^{14}NO_x^-\right]}{\Delta T} = \overline{F_3}\times(1-\overline{r_{NH_4^+}}) - \overline{F_4}\times(1-\overline{r_{NO_x^-}})$$

$$\frac{\Delta\left[{}^{14}PN\right]}{\Delta T} = \overline{F_1}\times(1-\overline{r_{NH_4^+}}) + \overline{F_4}\times(1-\overline{r_{NO_x^-}}) - \overline{F_5}\times(1-\overline{r_{PN}})$$

For the high nutrient complex case (NO_2^- and NO_3^- in separable pools), we indeed encountered equifinality problem in old version since we have 6 independent equations and 7 unknowns.

In previous version, we applied linear programming (Excel solver) to obtain the optimal solution for 7 unknowns. The non-linear GRG (Generalized Reduced Gradient Algorithm) was selected. The target function is the root mean square error for all six equations. When the value of target function reaches minimum the optimal solution was provided. After obtaining the optimal solution, we simulate time courses by using the constructed Stella model. Time course extrapolation provided by Stella were surprisingly good, thus, we overlooked the multimodel optimization problem pointed out by reviewer.

The old and revised model are shown below in (a) and (b), respectively, for high nutrient case. Similar to the simple case, in this version we removed F7, nitrite excretion (see panel (a) below in Figure r2). In high NH_4^+ estuary and coastal sea, nitrate assimilation may be inhibited in oxygenated water and subsequently, the nitrite release. Thus, the ignorance of nitrite release from PN (F7 in lower panel (a)) should be acceptable. In old version, equations for PN pool were not applied independently. In order to discuss the missing ammonium, we now introduced PN into equation set. Thereby, the number of total parameters is eight. With eight independent equations a unique parameter combination can be obtained (see equations below). During the revision, we compared with ODE-derived results (see reply to comment #3 above, new Table 2a). We also examined the sensitivity of parameters in accordance with the target function (see reply below to the last specific comment) and found all rates converged to unique solutions.

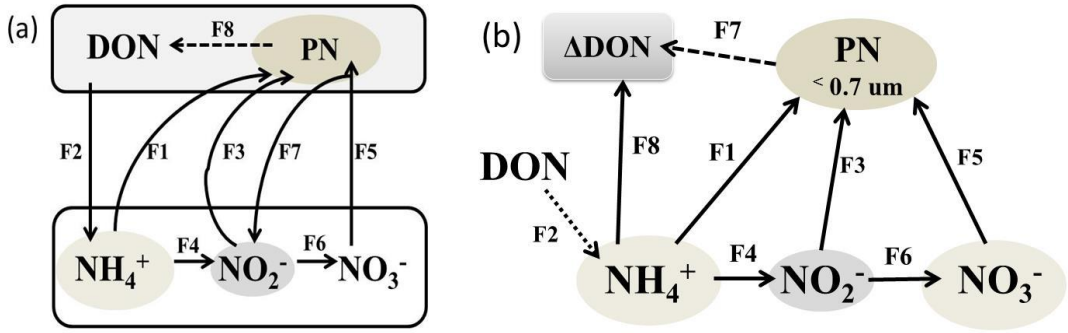

Figure r2. The old (a) and revised (b) model structures for high nutrient case.

Equations for the high nutrient case:

$$\frac{\Delta\left[{}^{15}NH_4^+\right]}{\Delta T} = \overline{F_2}\times 0.00366 - \overline{F_1}\times\overline{r_{NH_4^+}} - \overline{F_4}\times\overline{r_{NH_4^+}} - \overline{F_8}\times\overline{r_{NH_4^+}}$$

$$\frac{\Delta\left[{}^{15}NO_2^-\right]}{\Delta T} = \overline{F_4}\times\overline{r_{NH_4^+}} - \overline{F_3}\times\overline{r_{NO_2^-}} - \overline{F_6}\times\overline{r_{NO_2^-}}$$

$$\frac{\Delta\left[{}^{15}NO_3^-\right]}{\Delta T} = \overline{F_6}\times\overline{r_{NO_2^-}} - \overline{F_5}\times\overline{r_{NO_3^-}}$$

$$\frac{\Delta\left[{}^{15}PN\right]}{\Delta T} = \overline{F_1}\times\overline{r_{NH_4^+}} + \overline{F_3}\times\overline{r_{NO_2^-}} + \overline{F_5}\times\overline{r_{NO_3^-}} - \overline{F_7}\times\overline{r_{PN}}$$

$$\frac{\Delta\left[{}^{14}NH_4^+\right]}{\Delta T} = \overline{F_2}\times(1-0.00366) - \overline{F_1}\times(1-\overline{r_{NH_4^+}}) - \overline{F_4}\times(1-\overline{r_{NH_4^+}}) - \overline{F_8}\times(1-\overline{r_{NH_4^+}})$$

$$\frac{\Delta\left[{}^{14}NO_2^-\right]}{\Delta T} = \overline{F_4}\times(1-\overline{r_{NH_4^+}}) - \overline{F_3}\times(1-\overline{r_{NO_2^-}}) - \overline{F_6}\times(1-\overline{r_{NO_2^-}})$$

$$\frac{\Delta\left[{}^{14}NO_3^-\right]}{\Delta T} = \overline{F_6}\times(1-\overline{r_{NO_2^-}}) - \overline{F_5}\times(1-\overline{r_{NO_3^-}})$$

$$\frac{\Delta\left[{}^{14}PN\right]}{\Delta T} = \overline{F_1}\times(1-\overline{r_{NH_4^+}}) + \overline{F_3}\times(1-\overline{r_{NO_2^-}}) + \overline{F_5}\times(1-\overline{r_{NO_3^-}}) - \overline{F_7}\times(1-\overline{r_{PN}})$$

Our approach differs from that in Pfister et al. (2016), in which the ratio of ammonium uptake to nitrate uptake was fixed by trial and error. According to comments below and from other reviewers, we also presented additional case and discussed the light effect.

Specific comments

Line 47 – p3: What is meant by the inventory method?
Author response − We followed B. B. Ward (2011). We made a much clearer description. The sentence is now "The inventory method (monitoring substrate and/or product change over time) is often used …".

Line 100 – p6: The term validation is not appropriate since the Stella model is based on the reaction kinetics outlined in Fig.1, and thereby submitted to the same underlying hypotheses than Eqns (16-17). At best we can say that the matrix solutions

are consistent with a model run generating concentration versus time curves through back calculation.

Author response − We partly agree with reviewer. This question was raised due to the under-descriptions of our method. For both cases, the "instant rate" for the first time interval was obtained and then served as prescribed values in Stella box model to predict the time course and to compare with consecutive observations. Since the rate is concentration dependent (first order reaction), the rate constant derived from the first time interval would not guarantee a good performance for the full time course due to decline of substrate and contemporary community change. The extrapolation is a kind of validation.

In the ocean, the rate we are eager to know is the *in situ* rate (or the instant rate at the time of sampling) before microbial community changes. Thus, short-term incubation was suggested in our previous version. Stand on this point, "validation" is a proper term.

Lines 280/281/397/399/417. Please pay attention to the number of significant decimals when reporting data (e.g. 22.3± 4.3 μM or 5376.4 nM).

Author response − Carefully checked and corrected.

Line 348/354: How did the authors define 'undetectable' or 'below detection limit' in their ms?

Author response − We change to "below the detection limit".

Line 420 – p23: In Fig.4 a nonlinear behavior for the concentration versus time doesn't demonstrate that the rate laws follow first order.

Author response − Reviewer is correct. Now an assumption of first order reaction was made explicitly instead of by the judgement from apparent non-linear behavior.

Line 438 – p23: What is meant by 'this positive offset was compensated for by organic nitrogen utilization'.

Author response − We admit the old sentence was confusing. The sentence is now "Since both ammonium and NO_x^- fitted well within 12 hours, the extra non-fitted PN at the time point of 12 hours in observation likely indicated an additional nitrogen source, such as organic nitrogen, was utilized by phytoplankton when inorganic nitrogen reached threshold levels (Sunda and Ransom, 2007)." In fact, our flow cytometry data (see panel below) showed clearly the cell abundance of pico-eukaryotes increased within the first 24 hours and then decreased rapidly, very likely due to nutrient limitation. By contrast, the *Synechococcus* grew continuously even when ammonium and nitrate was around the limiting level. *Synechococcus* may thus uptake DON or recycled nitrogen for growth. Such result is not only supportive of the importance of short-term incubation also indicative of rate might change

rapidly due to community change.

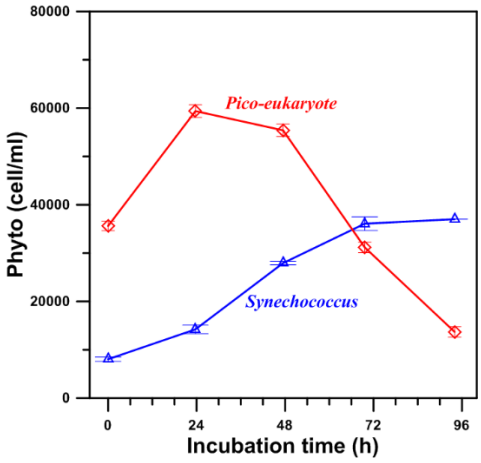

Figure r3. The variations of cell abundances of *Pico-eukaryote* and *Synechococcus* determined by flow-cytometry.

Line 518 – p27: I guess it is rather an 'accurate measurement of…'
Author response − Changed as suggested.

Line 544 – p 29: 'The uncertainty estimate for this isotope matrix method is not a simple statistical question'. Yet the authors have the means to do so. If they build rate profiles from their concentration measurements, and optimize values for Fi or ki (Eqns 16- 17) using a least squares method, they will get access to the uncertainty on these parameters via the variance-covariance matrix.
Author response – This question was raised due to more equations for unknowns. As replied above, after revision unique solution can be obtained via the matrix method. Thus, this specific uncertainty question does not exist. We mentioned uncertainties in previous version since we also cannot deny uncertainties caused by chemical analyses. Meanwhile, errors along the time course might possibly come from the community change as replied above.
According to this suggestion, we applied a sensitivity test (see Figure r4 below) by using Excel for the low nutrient case under r_{NH4+} constant condition. We set reasonable ranges for parameters and then conducted 10000 times random selection for individual parameters within the given range to generate 10000 sets of parameter combination for RMSE estimate. We can see clearly randomly selected parameters converge toward the unique solution we obtained (red inverse triangle). The RMSE is near zero. Such consistency suggests uncertainties will be sourced from chemical analyses and the heterogeneity of water for incubation rather than method itself.

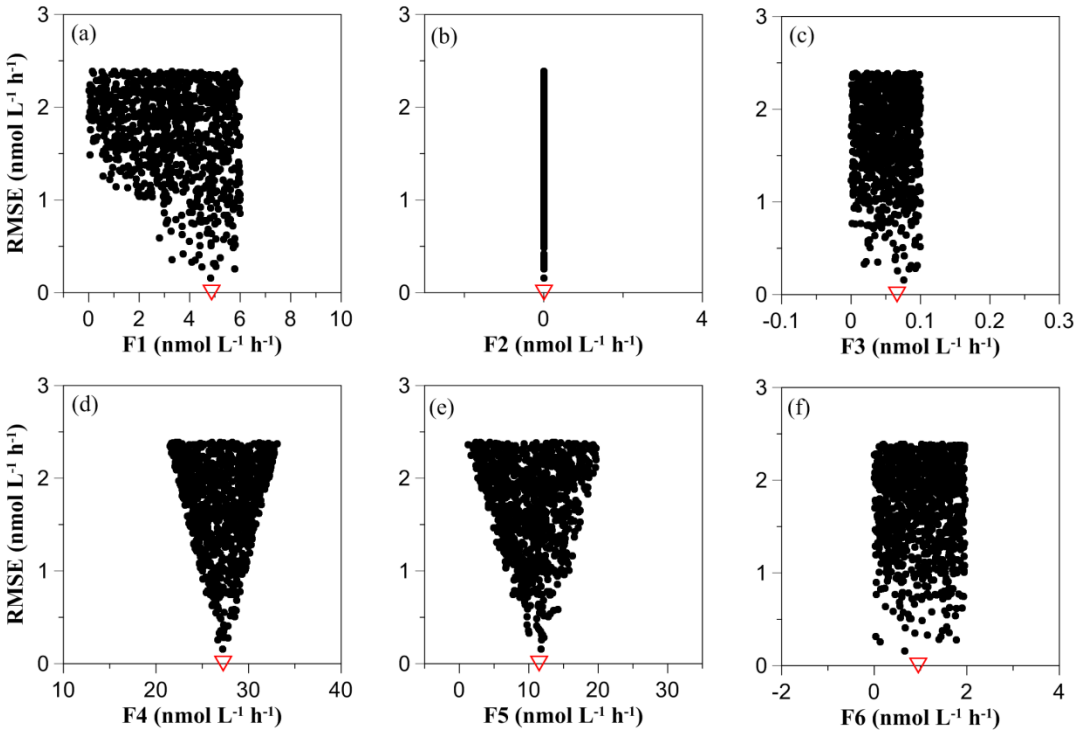

Figure r4. The sensitivity test of parameters. Root mean square error was applied as performance measure. Inverse triangle stands for unique solution from isotope matrix method.

Reviewer #3, Comment #1

The manuscript would be stronger if a wider range of environments with varying relative importance of the different processes were examined. At present, the manuscript really just addresses two incubation experiments taken from high light environments.

Author response:

The coastal case, in fact, we sampled two layers with different light intensity, 80% and 2% sPAR, and bottles were incubated in neutral density-screened incubator to simulate original light. In the old version, we did not presente entire data since the scope of this paper is to provide a convenient method.
According to this suggestion, we presented additional data. We saw higher rates of ammonium, nitrite and nitrate uptake for the high light layer. While nitrite and ammonium oxidation were both low compared with phytoplankton uptake. The overall low ammonium oxidation rate was likely attributable to the low temperature in winter. The amount of ammonium uptake by microbes was similar to that by phytoplankton in both cases underscoring the importance of ammonium flow to < 0.7 μm particle fraction.
We do not add further cases we have. Our next paper will be focusing on the application of this method to discuss the temperature and light effect on multiple processes in an estuary along salinity gradient.

Reviewer #3, Comment #2

The manuscript should include a deeper discussion of the results beyond just the new method, extending to the actual ecology of the processes being examined. For example, the finding that varying the remineralization rate does not affect the nitrification rate seems significant, though potentially an artifact of the samples chosen for investigation (see #1 above).

Author response:

We agree with reviewer, the results might be very different in other environments. We included the layer with 2% sPAR for discussion. According to this comment, we modified the model structure (see reply to comment #4 by Reviewer #2) to discuss the missing ammonium. In old version, the unbalanced nitrogen was assigned as a leakage to DON from PN. As indicated in our manuscript, PON was operationally defined (on GF/F filter pore size of 0.7 μm). The nitrogen leakage, in fact, had been observed elsewhere. As pointed out by Laws (1985), the leakage from PON to DON

or bacterial ammonium uptake (<0.7μm, absence on filter) may account for the vanishing $^{15}NH_4^+$ on PON. In this version, we separated the missing nitrogen into account for the vanishing ammonium in incubation bottle. Thus, variable remineralization rate (variable r_{NH4+}) was assigned to test the dilution effect.
Basing on our observational data, the continuously decreasing ammonium over time was obvious, suggesting that remineralization was insufficiently high to maintain the ammonium at steady state. Such rapid drop in ammonium was supportive of low remineralization rate deduced from time course extrapolation. As indicated by Pfister et al. (2016), benthic mussels play a critical role in ammonium supply in tidal ponds. In our both cases, micro-zooplankton in sampled water may not present in high abundance. Limited zooplankton (animals) in sampled water is likely the key for insignificant remineralization. More discussions will be made for ecological implications.

Specific comments

There is an over emphasis on the novelty of this work being 'abandoning inhibitors', as most stable isotope labeling papers in the last decade have not used inhibitors to actually calculate rates, but rather to inform specific groups of organisms that might be contributing to a specific process. This is the case for many of the papers incorrectly cited in lines 61-63.
Author response − We do not mention 'abandoning inhibitors' in this version. References were carefully checked and cited accordingly.

80% surface light intensity is a very high light intensity for trying to measure nitrification. I would suggest noting in the discussion that the contribution from nitrification to ^{15}N uptake might be considerably different at lower (e.g. 1-10%) surface irradiance. This is somewhat alluded to in lines 381-384, but the implications could be discussed more explicitly.
Author response − We totally agree with this comment. We provide low light case in this version. However, nitrification rate was still low due to low temperature in winter. We described the light effect on nitrification and referred to papers about light inhibition and substrate competition (Smith et al. 2014; Peng et al. 2016). We also explicitly stated these flows or rates in low light environment could be very different from results we presented in this study.

Line 539: Are rates (nmol L^{-1} h^{-1}) or rate constants (h^{-1}) being compared here? Clarify language. Also, the phrase 'their nitrate uptake rate' is confusing . . .I think what is meant is 'nitrate uptake calculated using their method'
Author response − Corrected. All units in tables were carefully checked. Both rate values and rate constant will be presented clearly.

Line 562: The discussion about the relevance of this research to PNM dynamics is not warranted based on the results presented here.
Author response −We removed PNM relevant discussions.

Table 3: The column title ‘Santoro et al.’ should be clarified to say ‘Rate calculation of Santoro et al’ and units should be clarified for all columns (see comment above about rates versus rate constants). Table 2 has the NOx uptake rate constant (k) as 0.059 h^{-1}, but this same value is listed as a rate (nM h^{-1}) in Table 3.
Author response − The column title is corrected. We carefully checked for rate and rate constants throughout the manuscript and tables. The units and associated descriptions are now consistent.

Line 57: ‘manily’ should be ‘mainly’.

Author response − Corrected.

Line 182: is sulfamic, not sulfanilic meant here?
Author response − Corrected.

Line 482: ‘resut’ should be ‘result’.
Author response − Corrected.

Quantification of multiple simultaneously occurring nitrogen flows in the euphotic ocean

Min Nina Xu[1], Yanhua Wu[2], Li Wei Zheng[1], Zhenzhen Zheng[1], Huade Zhao[3], Edward A Laws[4], Shuh-Ji Kao[1]*

[1]State Key Laboratory of Marine Environmental Science, Xiamen University, Xiamen, China

[2]Shenzhen Marine Environment Monitoring Center Station, Shenzhen, China

[3]National Marine Environmental Monitoring Center, Dalian, China

[4]School of the Coast & Environment, Louisiana State University, USA

Correspondence to: Shuh-Ji Kao (sjkao@xmu.edu.cn)

Abstract

The general features of the N cycle in the sunlit ocean have been recognized, but quantitative information about multiple transformation rates among nitrogen pools, i.e., ammonium (NH_4^+), nitrite (NO_2^-), nitrate (NO_3^-) and particulate/dissolved organic nitrogen (PN/DON), are insufficient due to methodological difficulties. Recent advances in analytical methods for isotopic composition of oft-measured nitrogen species allowed us to establish a convenient isotope labelling method to quantify *in situ* dynamic nitrogen flows for euphotic water. By adding a single ^{15}N-labelled NH_4^+ tracer, we monitored the changes in concentration and isotopic composition of the total dissolved nitrogen (TDN), PN, NH_4^+, NO_2^-, and NO_3^- pools to trace the ^{15}N and ^{14}N flows. Based on mass and isotope conservations of every individual pool as well as the whole system, we formulated matrix equations with unique solution to simultaneously derive multiple nitrogen transformation rates, such as rates of NH_4^+, NO_2^-, and NO_3^- uptake; ammonia oxidation; nitrite oxidation; DON release and NH_4^+ uptake by bacteria. This isotope matrix method was designed specifically for euphotic water column incubation under simulated *in situ* condition. With consideration of multi-flows among pools, we minimized potential biases caused by non−targeted processes in traditional source-product method. The proposed isotope matrix method is convenient in terms of on-deck incubation and post-hoc data analysis and is feasible to probe

effects of environmental factors (e.g., pH, temperature and light) on multiple processes under manipulated conditions.

Keywords

Ammonium oxidation, isotope, new production, nitrification, regenerated production

1. Introduction

Nitrogen (N), which is an essential element in organisms' metabolic processes, regulates productivity in the surface waters of many parts of the ocean (Falkowski, 1997; Zehr and Kudela, 2011; Casciotti, 2016). As a limiting nutrient in the euphotic zone, nitrogen rapidly interconverts among five major N compartments: particulate organic nitrogen (PN), dissolved organic nitrogen (DON), ammonium (NH_4^+), nitrite (NO_2^-), and nitrate (NO_3^-) (Fig. 1). Quantitative information on transformation rates in the marine N-cycle may advance our understanding of the coupling of autotrophic and heterotrophic processes involving carbon and nitrogen as well as the efficiency of the biological pump. Such information would also facilitate evaluation of ecosystem functions. However, the dynamic nature and complexity of the reactions involving nitrogen make it a difficult task to resolve the rates of multiple simultaneous nitrogen transformations. Inventory and isotope tracer methods have often been used to measure rate of specific process in previous studies (Ward, 2008, 2011; Lipschultz, 2008 and references therein).

The inventory method (monitoring the change of substrate and/or product concentrations over time) was often used to determine the uptake rates of ammonium, nitrite, nitrate, and urea (McCarthy and Eppley, 1972; Harvey and Caperon, 1976; Harrison and Davis, 1977; Howard et al., 2007) and to examine the occurrence and rate of nitrification (Wada and Hatton, 1971; Pakulski et al., 1995; Ward, 2011). However,

unwanted processes may bias the result. For example, the substrate (ammonium) pool is controlled simultaneously by consumptions via phytoplankton (PN as the product), nitrifier (nitrite/nitrate as the product) and bacteria (operationally defined DON as product) and by additions via remineralization from heterotrophic bacterial metabolism, zooplankton excretion, and viral lysis. Similarly, the product (NO_x^-) pool of nitrification is consumed contemporarily by phytoplankton during incubation.

The ^{15}N-labeled tracer technique has been widely used as a direct measure for specific nitrogen processes since the emergence of isotope ratio mass spectrometry (IRMS). For example, the addition of ^{15}N-labeled nitrate has been applied to estimate new production (Dugdale and Goering, 1967; Chen, 2005; Painter et al., 2014). Likewise, by incubating water to which $^{15}NH_4^+$ has been added, nitrification rate ($^{15}NO_3^-$ as product; e.g. Newell et al., 2013; Hsiao et al., 2014; Peng et al., 2016) and ammonium uptake rate ($^{15}N_{PN}$ as product; e.g. Dugdale and Goering, 1967; Dugdale and Wilkerson, 1986; Bronk et al., 1994, 2014) can be measured, respectively, with dark and light incubation. However, isotope-labelling encounters similar bias problem in the inventory method, i.e., multiple processes occur simultaneously involving either source or product terms in the incubation bottle. In fact, these transformations among pools have significant implications in biogeochemical cycle. For instance, Yool et al. (2007) synthesized available global data and indicated that the fractional contribution of nitrate derived from nitrification to nitrate uptake can be as high as 19–33% in the

euphotic zone. However, nitrate uptake rates were determined under light conditions, and nitrification was determined under dark conditions (e.g. Grundle et al., 2013), which are not comparable in terms of their effects on these processes. To overcome this problem, 24-h incubations have been used to compensate for the diel cycle of light-sensitive processes (Beman et al., 2012). Yet, 24-h incubations may cause calculation artifacts due to the interference from significant transfers of ^{15}N and ^{14}N among pools. A new method is needed to reconcile the above-mentioned biases and the incomparable parallel incubations.

Marchant et al. (2016) have reviewed recent method advances in marine N-cycle studies using ^{15}N-labeling substrates combined with nanoSIMS, FISH, or HISH. These methods provide qualitative information for N transfers at cellular and molecular level but no quantitative rates at community level. A comprehensive review of oft-used models for rate derivation was conducted by Elskens et al. (2005), who concluded that oversimplified models would risk bias when their underlying assumptions are violated; nevertheless, overly complex models could misinterpret part of the random noise as relevant processes. Therefore, a model selection procedure was subsequently proposed (De Brauwere et al., 2005). More recently, Pfister et al. (2016) applied isotope tracer technique and mass conservation model onto tidal ponds study to explore nitrogen flows among dissolved nitrogen pools (NH_4^+, NO_2^- and NO_3^-) and found that benthic macrobiota plays important role in regulating remineralization flow. They also proved

that the dilution effect significantly biased the results obtained by source-product models. Nevertheless, for the euphotic zone where competing processes co-occur, an innovative and convenient method for on-deck incubation to measure *in situ* multiple N flows is needful.

In this study, we propose an "isotope matrix method". To avoid perturbations, the concentration of the tracer was limited to < 10% or 20 % of the substrate concentration, as suggested by previous researchers (Raimbault and Garcia, 2008; Middelburg and Nieuwenhuize, 2000; Painter et al., 2014). One single tracer, $^{15}NH_4^+$, was added into incubation bottle to trace the ^{15}N flow among the nitrogen pools under simulated *in situ* conditions. Almost all the most fundamental processes in the N cycle can be quantified with this newly proposed method. To demonstrate the applicability of the method, we conducted incubation experiments for low-nutrient water in the western North Pacific and for high-nutrient coastal water off southeastern China coast. Thank for recent advances in these analytical methods for concentration and isotopic composition of various nitrogen species, this isotope matrix method becomes applicable to quantify *in situ* dynamic nitrogen flows for euphotic water.

2. Isotope matrix method

2.1 Framework of the inter-connections among nitrogen pools

In the oxygenated and well-lit euphotic zone, the transformations of N among NH_4^+, NO_2^-, NO_3^-, PN, and DON are shown in Fig. 1. The PN is operationally defined

as the particulate organic nitrogen trapped on a GF/F filter (> 0.7μm). Dissolved inorganic nitrogen (DIN) and DON are the inorganic and organic nitrogen, respectively, in the dissolved fraction that passes through a polycarbonate membrane with a 0.22 μm pore size. Since DON includes the N in numerous dissolved organic N compounds, including unidentified organics, urea, amino acids, amines, and amides, DON represents the "bulk" DON and is calculated by subtracting the concentrations of NH_4^+, NO_2^-, and NO_3^- (DIN) from the total dissolved N (TDN).

We consider two different types of schemes in our method: low nitrogen and high nitrogen (Fig. 1a and 1b). The low nutrient scheme is for the open ocean. The high nutrient scheme is for estuary and coastal environments where three dissolved inorganic nitrogen species co-exist. Below, we describe the rationale of model structures for the two cases.

The consumption of reactive inorganic nitrogen (NH_4^+, NO_2^-, and NO_3^-) is dominated by photosynthetic uptake by phytoplankton (F1 and F4 in Fig. 1a; F1, F3, and F5 in Fig. 1b). Heterotrophic bacteria may also be important actors for NH_4^+ assimilation (Laws, 1985), and was confirmed by studies later on (e.g. Middelburg and Nieuwenhuize, 2000; Veuger et al., 2004). We took it into account as well (F6 in Fig. 1a and F8 in Fig. 1b) to explore its importance. Though NO_2^- may be released during NO_3^- uptake (Lomas and Lipschultz, 2006), little NO_2^- production from NO_3^- was detected (Santoro et al., 2013), especially in high NH_4^+ estuary and coastal sea, nitrate

assimilation may be inhibited in oxygenated water and, subsequently, so is the nitrite release. Thus, the nitrite release was ignored in our model. Due to DIN assimilation by phytoplankton, the PN pool may increase, but DON may be released during assimilation (F5 in Fig. 1a and F7 in Fig. 1b) as indicated by previous studies (Bronk et al., 1994; Bronk and Ward, 2000; Varela et al., 2005). On the other hand, remineralization may refuel the NH_4^+ pool (F2 in both Fig. 1a and 1b). Meanwhile, ammonium pool is reduced by nitrification process, which consists of two basic steps: the ammonia oxidation by archaea/bacteria (AOA/AOB) to nitrite (F4 in Fig. 1b) and the nitrite oxidation to nitrate by nitrite-oxidizing bacteria (NOB) (F6 in Fig. 1b). Although recent studies have revealed a single microorganism that may completely oxidize NH_4^+ to NO_3^- (comammox) (Daims et al., 2015; van Kessel et al., 2015), its importance in the marine environment remains unclear.

Specific mechanisms or processes such as grazing and viral lysis may alter the concentrations of NH_4^+, nitrite, and DON. However, the scope of this study is to determine the nitrogen flows and exchanges among the often measured and operationally defined nitrogen pools. In this context, grazers and viruses belong to the operationally defined PN and DON pools, respectively. Thus, the resultance of specific process such as grazing and viral lysis has been incorporated in the paradigm depicted in Figure 1.

2.2 Analytical methods to determine the amounts of $^{15}N/^{14}N$ in various pools

To trace the ^{15}N movement among pools, our isotope matrix method couples the ^{15}N-labelling and inventory methods through considering both concentration and isotopic composition changes. Analytical methods to determine the concentrations and isotopic compositions of both high and low levels of inorganic/organic nitrogen are in most cases well established and have been reported elsewhere. We determined all of the mentioned concentrations and isotopic compositions except the isotopic composition of NH_4^+.

Concentrations of NH_4^+ higher than 0.5 μM were measured manually by using the colorimetric phenol hypochlorite technique (Koroleff, 1983). Nanomolar NH_4^+ concentrations were measured by using the fluorometric o-phthaldialdehyde (OPA) method (Zhu et al., 2013). Concentrations of NO_2^- and NO_x^- (NO_2^- + NO_3^-) were determined with the chemiluminescence method following the protocol of Braman and Hendrix (1989). The detection limits of NO_2^- and NO_x^- were both ~ 10 nmol L^{-1}, and the corresponding relative precision was better than 5% within the range of concentrations that we measured. By using persulfate as an oxidizing reagent, we oxidized TDN and PN separately to nitrate (Knapp et al., 2005) and then measured the nitrate by using the analytical method for NO_x^- described above.

We determined the $\delta^{15}N$ of NO_2^- with the azide method by following the detailed procedures in McIlvin and Altabet (2005). The $\delta^{15}N$ of NO_x^- was determined by using a distinct strain of bacteria that lacked N_2O reductase activity to quantitatively convert

176 NO_x^- to nitrous oxide (N_2O), which we then analyzed by IRMS (denitrifier method;
177 (Sigman et al., 2001; Casciotti et al., 2002). The isotopic composition of NO_3^- was
178 determined from isotope mass balance (NO_x^- minus NO_2^-) or measured by the
179 denitrifier method after eliminating preexisting NO_2^- with sulfamic acid (Granger and
180 Sigman, 2009). To determine the $\delta^{15}N$ of TDN and PN, both species were first
181 converted to NO_3^- with the denitrifier method, and then the $\delta^{15}N$ of the NO_3^- was
182 determined as described above. The detection limit of $\delta^{15}N_{PN}$ can be reduced to
183 nanomole level (absolute amount of nitrogen), which is significantly lower than that
184 by using high temperature combustion with an elemental analyzer connected to
185 IRMS.

186 The most popular way to determine the N isotopic composition of NH_4^+ is the
187 "diffusion method", which involves conversion of dissolved NH_4^+ to NH_3 gas by
188 raising the sample pH to above 9 with magnesium oxide (MgO) and subsequently
189 trapping the gas quantitatively as $(NH_4)_2SO_4$ on a glass fiber (GF) filter; the isotope
190 ratios of the $^{15}N/^{14}N$ are then measured using a coupled elemental analyzer with an
191 IRMS (Holmes et al., 1998; Hannon and Böhlke, 2008). Alternatively, after removing
192 the preexisting NO_2^- from the seawater samples using sulfamic acid, NH_4^+ is first
193 quantitatively oxidized to NO_2^- by hypobromite (BrO^-) at pH ~12 (BrO^- oxidation
194 method), and the protocol of McIlvin and Altabet (2005) is then used to reduce the
195 NO_2^- to N_2O (Zhang et al., 2007). Unfortunately, neither of these methods has been

196 established in our lab yet. The isotope matrix method requires the isotopic composition
197 of NH_4^+ as well, but this requirement can be circumvented by making certain
198 assumptions, as illustrated in our case studies below.

199 We estimated the amount of ^{14}N and ^{15}N atoms in every individual pool for which
200 we knew the concentration and $\delta^{15}N$ ($\delta^{15}N$ ‰ = $[(R_{sample} - R_{atmN2})/R_{atmN2}] \times 1000$). By
201 assuming the ^{15}N content of standard atmospheric nitrogen to be 0.365%, we calculated
202 R_{sample} ($^{15}N/^{14}N$). By defining r_{sample} as $^{15}N/(^{14}N+^{15}N)$, we directly derived the ^{15}N and
203 ^{14}N concentrations of all forms of N, with the exception of NH_4^+ and DON. The r value
204 of the NH_4^+ was assumed to equal either its initial value or an arbitrarily chosen fraction
205 thereof, and the ^{15}N and ^{14}N content of the NH_4^+ was then determined.

206 **2.3 Formation of matrix equations**

207 In this isotope matrix method, we added limited amount of $^{15}NH_4^+$ into incubation
208 bottles at the very beginning and then monitored the changes of ^{15}N and ^{14}N in the
209 measured pools every a few hours. We assumed isotopic mass balance at every time
210 point in the incubation bottle. In other words, the sums of the variations in the total N,
211 ^{15}N, and ^{14}N concentrations were zero for any time interval. We assumed no
212 fractionation between ^{15}N and ^{14}N for all the transfer reactions among the pools. The
213 fluxes of ^{15}N and ^{14}N were therefore equal to the total flux multiplied, respectively, by
214 $r_{substrate}$ and $(1 - r_{substrate})$. Note that we did not consider isotope fractionation, though it
215 could easily be introduced into the equations if necessary, i.e., dividing ^{14}N flux by α

(the ratio of specific rate constant of ^{14}N to ^{15}N), and the flux of ^{15}N is obtained. Below, we illustrated equations for the two model cases.

According to mass balance, the net changes of the ^{15}N (or ^{14}N) concentration of individual N pool in certain time interval are determined by the inflow and outflow of ^{15}N (or ^{14}N) (see Fig. 1 and Eqs. below). In the low-nitrogen case, the changes of the ^{15}N concentrations of the NH_4^+, NO_x^-, and PN pools were expressed by Eq. 1, 2 and 3, respectively. Similarly, the temporal dependence of ^{14}N-NH_4^+, ^{14}N-NO_x^-, and ^{14}N-PN were expressed by Eq. 4, 5 and 6, respectively. The mean rate of change in nitrogen pool, i.e. the left side of the equation, was determined from the data at time zero and the first time point. For example, when sampling time interval is short, $\Delta[^{14}NH_4^+]/\Delta t$ at the first time point was approximately $\{[^{14}NH_4^+]_{t1} - [^{14}NH_4^+]_{t0}\}/(t1-t0)$ where the subscripts indicate the times at which the concentrations were measured. The r value applied in the equation for substrate was the average of the r values at time zero and the first time point after that for measured pool.

$$\frac{\Delta\left[{}^{15}NH_4^+\right]}{\Delta T} = \overline{F_2} \times 0.00366 - \overline{F_1} \times \overline{r_{NH_4^+}} - \overline{F_3} \times \overline{r_{NH_4^+}} - \overline{F_6} \times \overline{r_{NH_4^+}} \quad (1)$$

$$\frac{\Delta\left[{}^{15}NO_x^-\right]}{\Delta T} = \overline{F_3} \times \overline{r_{NH_4^+}} - \overline{F_4} \times \overline{r_{NO_x^-}} \quad (2)$$

$$\frac{\Delta\left[{}^{15}PN\right]}{\Delta T} = \overline{F_1} \times \overline{r_{NH_4^+}} + \overline{F_4} \times \overline{r_{NO_x^-}} - \overline{F_5} \times \overline{r_{PN}} \quad (3)$$

$$\frac{\Delta\left[{}^{14}NH_4^+\right]}{\Delta T} = \overline{F_2}\times(1-0.00366) - \overline{F_1}\times(1-\overline{r_{NH_4^+}}) - \overline{F_3}\times(1-\overline{r_{NH_4^+}}) - \overline{F_6}\times(1-\overline{r_{NH_4^+}}) \quad (4)$$

$$\frac{\Delta\left[{}^{14}NO_x^-\right]}{\Delta T} = \overline{F_3}\times(1-\overline{r_{NH_4^+}}) - \overline{F_4}\times(1-\overline{r_{NO_x^-}}) \quad (5)$$

$$\frac{\Delta\left[{}^{14}PN\right]}{\Delta T} = \overline{F_1}\times(1-\overline{r_{NH_4^+}}) + \overline{F_4}\times(1-\overline{r_{NO_x^-}}) - \overline{F_5}\times(1-\overline{r_{PN}}) \quad (6)$$

In this study, we conducted a time series monitoring for over 24 hours, however, we took the first two time points for the rate calculation since such rate derivations might be more close to the instant rates in the original environments. Note: researchers may apply this method onto longer time interval, however, rates may vary as a result of substrate consumption and/or community change, shorter-term incubation is suggested (see below).

Since the total number of equations and unknowns are equal, a unique solution therefore can be obtained via matrix solution for the low nutrient model.

In high nutrient cases, similarly, equations (Eqs. 7-14) can be constructed by using transformations among NH_4^+, NO_2^-, NO_3^- and PN (Fig. 1b).

$$\frac{\Delta\left[{}^{15}NH_4^+\right]}{\Delta T} = \overline{F_2}\times 0.00366 - \overline{F_1}\times\overline{r_{NH_4^+}} - \overline{F_4}\times\overline{r_{NH_4^+}} - \overline{F_8}\times\overline{r_{NH_4^+}} \quad (7)$$

$$\frac{\Delta\left[{}^{15}NO_2^-\right]}{\Delta T} = \overline{F_4}\times\overline{r_{NH_4^+}} - \overline{F_3}\times\overline{r_{NO_2^-}} - \overline{F_6}\times\overline{r_{NO_2^-}} \quad (8)$$

$$\frac{\Delta\left[{}^{15}NO_3^-\right]}{\Delta T} = \overline{F_6}\times\overline{r_{NO_2^-}} - \overline{F_5}\times\overline{r_{NO_3^-}} \quad (9)$$

$$\frac{\Delta\left[{}^{15}PN\right]}{\Delta T} = \overline{F_1} \times \overline{r_{NH_4^+}} + \overline{F_3} \times \overline{r_{NO_2^-}} + \overline{F_5} \times \overline{r_{NO_3^-}} - \overline{F_7} \times \overline{r_{PN}} \quad (10)$$

$$\frac{\Delta\left[{}^{14}NH_4^+\right]}{\Delta T} = \overline{F_2} \times (1-0.00366) - \overline{F_1} \times (1-\overline{r_{NH_4^+}}) - \overline{F_4} \times (1-\overline{r_{NH_4^+}}) - \overline{F_8} \times (1-\overline{r_{NH_4^+}}) \quad (11)$$

$$\frac{\Delta\left[{}^{14}NO_2^-\right]}{\Delta T} = \overline{F_4} \times (1-\overline{r_{NH_4^+}}) - \overline{F_3} \times (1-\overline{r_{NO_2^-}}) - \overline{F_6} \times (1-\overline{r_{NO_2^-}}) \quad (12)$$

$$\frac{\Delta\left[{}^{14}NO_3^-\right]}{\Delta T} = \overline{F_6} \times (1-\overline{r_{NO_2^-}}) - \overline{F_5} \times (1-\overline{r_{NO_3^-}}) \quad (13)$$

$$\frac{\Delta\left[{}^{14}PN\right]}{\Delta T} = \overline{F_1} \times (1-\overline{r_{NH_4^+}}) + \overline{F_3} \times (1-\overline{r_{NO_2^-}}) + \overline{F_5} \times (1-\overline{r_{NO_3^-}}) - \overline{F_7} \times (1-\overline{r_{PN}}) \quad (14)$$

Again, a unique solution can be obtained since the numbers of equations and unknowns are equal.

In the above matrix equations, r_{NH4+}, which we did not measure in this study, is necessary for the solution. Here we set various degrees of remineralization to test the effect of isotope dilution (NH_4^+ addition) in our experimental cases. We reduced r_{NH4+} values at a constant reduction rate and the total reduction of r_{NH4+} was 0%, 1%, 10%, 20% and 50% for the full time span of incubation (r_{NH4+} of remineralization is assumed to be 0.00366). The F2 coupled with given r_{NH4+} values allowed us to resolve rates under different remineralization conditions, and the derived F2 was introduced into STELLA model for extrapolations (see below). We compared the observed and

264 remineralization-associated simulations to reveal the effect of remineralization on rate
265 measure for time series incubations.

266 **2.4 Validation by STELLA**

267 As the aforementioned, the "instant rate" at the original condition is what
268 researchers pursue. Note that the use of "instant" here is just to make it distinguishable
269 from the longer time incubation or more than two time points. To evaluate the
270 applicability of matrix-derived instant rate, here we applied STELLA 9.1.4 software
271 (Isee systems, Inc.) to construct box models that were consistent with the scenarios
272 depicted in Figure 1. The constructed STELLA model contained two modules (Figs. S1
273 and S2), one for ^{15}N and the other for ^{14}N. The connection between these two modules
274 was through the ^{15}N atom % (rN), which was a measured parameter in the incubation
275 experiment. The model started to run with these measured initial values for nitrogen
276 pools at time zero and to project continuous changes of corresponding nitrogen pools.
277 Since the rate numbers based on the first two time points may not guarantee a good
278 performance for the full time course due to system variation, i.e., changes in substrate
279 concentration and microorganism community, we took this model practice
280 (extrapolation) as a validation.

281 In this study, we assumed the first order reaction for both cases, thus, the initial
282 rate constant "k" can be derived via dividing matrix-derived F by $\bar{C}$ (the average
283 substrate concentration of the first two time points). After setting the initial

concentrations of ^{15}N and ^{14}N to every pool, the model ran for 24 h according to matrix-derived short-term k values. As depicted in Figure 1, all these monitored N pools are regulated by F, which is concentration dependent according to our assumption (Figs. S1 and S2). The output includes the time courses of the ^{15}N and ^{14}N concentrations and the ^{15}N atom % (r_N) of each N species. Through this comparison, we could observe the course evolution of the isotopic composition in various N pools.

2.5 Study sites and incubation experiments

Incubation experiments were conducted in two environments with very different nutrient levels. The low nutrient case was conducted on-deck of the R/V Dongfanghong 2 on a cruise to the Western North Pacific (WNP) (33.3 °N, 145.9 °E) in spring 2015. The site for the high nutrient case is in the Wuyuanwan Bay (WYW) (24.5 °N, 118.2 °E) in the southern coast of China.

The water samples at WNP station were collected using a 24-bottle rosette sampler. The sampling depth was 25 m with moderate light intensity (12% the surface water irradiance). Two pre-washed 10-L polycarbonate carboys (Nalgene, USA) were used for the incubation. A total of 1.5 mL of 200 μM ^{15}N-labelled NH_4Cl tracers containing 98 atom% 15N (Sigma-Aldrich, USA) was injected into each incubation bottle separately to achieve a final concentration of 30 nM. Incubation was carried out immediately with a constant simulated light intensity (35 μmol E m^{-2} s^{-1}) in a thermostatic incubator (GXZ-250A, Ningbo) at *in situ* temperature.

The WYW station is an inner bay with a regular semidiurnal tide. As a coastal bay, Wuyuanwan suffers from anthropogenic influences that result in high nutrient concentrations analogous to other coastal zones in China. However, the bay water is still well ventilated and constantly saturated with dissolved oxygen due to tidally induced water exchange. It is an ideal research site to study the dynamic transformation processes of the coastal nitrogen cycle.

The WYW samples were taken on 19 January, 2014 from water depth of 0.3 m and 2.3 m, respectively, with a light intensity of 80 % and 2% of the surface water irradiance. Duplicate water samples were collected for each depth by using submersible pump into pre-washed 10-L polycarbonate bottles (Nalgene, USA). ^{15}N-labeled NH_4Cl (98 atom % ^{15}N, Sigma-Aldrich, USA) was added to the incubation bottles with final concentration of 1 μM (~4 % of the ambient concentration). The incubations were carried out immediately in the field. Neutral density-screen that allows 80% and 2% light penetration was applied, respectively, for incubation bottles of shallow and deep samples. The temperature was maintained at ~13.7 ℃ by continuously pumped seawater throughflow.

Sample of the first time point (t0) was taken immediately after tracer addition. Subsequent samples were taken at approximately 2–4 h interval for DIN and PN analyses. An aliquot of 200 mL was filtered through a 47-mm polycarbonate membrane with a 0.22 μm pore size (Millipore, USA), and the filtrates were frozen at –20 ℃ for

chemical analyses in the lab. Particulate matter was collected by filtering 500 ml seawater through pre-combusted (450 ℃ for 4 h) 25 mm GF/F filters (Whatman, GE Healthcare, USA), under a pressure of <100 mm Hg. The GF/F filters were freeze-dried and stored in a desiccator for PN concentration and isotopes.

3. Results

3.1 Ambient condition and initial concentrations

The water temperature and salinity of the WNP low nutrient case from 25m was 18.4 ℃ and 34.8, respectively. The dissolved oxygen (DO) was 7.3 mg L^{-1}. The concentration of NH_4^+, NO_x^- and phosphate was 113 ± 5 nmol L^{-1}, 521 ± 18 nmol L^{-1} and 74 ± 2 nmol L^{-1}, respectively. The N/P ratio was lower than 16, indicating the system is N limited.

The water temperature and salinity of the WYW whole water column for high nutrient case was 13.5 ± 0.1 ℃ and 29.5 ± 0.1, respectively. The DO saturation ranged 135-140%. The concentrations of nitrogenous species were relatively high with inorganic nutrient concentrations of 30.9 ± 0.7 μmol L^{-1} for NO_3^-, 22.3 ± 4.3 μmol L^{-1} for NH_4^+, 5.4 ± 0.2 μmol L^{-1} for NO_2^-, and 9.3 ± 0.7 μmol L^{-1} for PN. Phosphate was 1.5 ± 0.1 μmol L^{-1}.

3.2 Time-courses of incubations

3.2.1 Low nutrient case

343 The observed variation patterns for the bulk NH_4^+, NO_x^-, PN, and TDN
344 concentrations and $\delta^{15}N$ of NO_x^- and PN during incubation are shown in Figure 2.
345 Concentrations of NH_4^+ and NO_x^- decreased rapidly from 143 ±5 to 48 ±5 nM and 521
346 ± 18 to 127 ± 11 nM, respectively (Figs. 2a and 2b). In contrast, PN concentration
347 increased from 437 ±9 to 667 ±14 nM (Fig. 2c), and the TDN concentration remained
348 stable, with an average of 6511 ± 209 nM (Fig. 2d). Opposite to the trend of NO_x^-
349 concentration, $\delta^{15}N$-NO_x^- increased from 8.9 ±0.2 to 171 ±2 ‰ (Fig. 2e). In addition,
350 $\delta^{15}N$-PN exhibited great changes, increasing from 46.8 ±0.2 to 6950 ±314 ‰ (Fig. 2f).

351 **3.2.2 High nutrient cases**

352 The time-series of observational parameters for samples from depths of 80% and 2%
353 sPAR exhibited similar variation trends during incubation (Fig. 3). During the course of
354 incubation, NH_4^+ decreased significantly and continuously from 26.6 ± 0.1 (initial
355 concentration) to 17.4 ±0.1 μmol L^{-1} with a mean reduction rate of 0.63 μmol L^{-1} h^{-1}
356 for 80% sPAR sample (Fig. 3a). Compared with that of 80% sPAR, NH_4^+ of 2% sPAR
357 sample decreased slower from 24.6 ±0.1 (initial concentration) to 18.2 ±1.0 μmol L^{-1}
358 with a mean reduction rate of 0.47 μmol L^{-1} h^{-1} (Fig. 3a). NO_3^- in 80% and 2% sPAR
359 decreased from 30.1 ±0.1 to 28.3 ±0.1 μmol L^{-1} and from 31.1 ±0.1 to 29.7 ±0.1 μmol
360 L^{-1}, respectively (Fig. 3c). Overall, the nitrate reduction rates were much lower than
361 that of NH_4^+. Compared to nitrate, NO_2^- displayed even slower declining trends yet
362 with significantly higher rate for 80% sPAR sample relative to that of 2% sPAR sample

363 (Fig. 3b). Similar to the low nutrient case, PN increased steadily from 8.8 ±0.1 to 17.7
364 ±0.9 μmol L^{-1} with a mean rate of 0.61 μmol L^{-1} h^{-1} for 80% sPAR sample and from
365 9.9 ±0.1 to 16.0 ±2.0 μmol L^{-1} with a mean rate of 0.44 μmol L^{-1} h^{-1} in 2% sPAR (Fig.
366 3d). The increase rates in PN concentration were very close to the decrease rates of
367 NH_4^+ indicating ammonium was the major nitrogen source for growth. The TDN
368 concentration decreased from 78.7 ±1.6 to 68.4 ±0.1 μmol L^{-1} and form 72.8 ±2.5 to
369 67.1 ±0.8 μmol L^{-1} for 80% and 2% sPAR samples, respectively (Fig. 3e).
370 The $\delta^{15}N\text{-}NO_2^-$ increased from –9.0 ±0.1 to 12.1 ±0.1 ‰ and –8.8 ±0.1 to 23.3 ±
371 0.6 ‰ in 80% and 2% sPAR incubation, respectively (Fig. 3g); Since nitrate pool was
372 relatively large, the values of $\delta^{15}N\text{-}NO_3^-$ ranged from 6.8 to 10.1 ‰ with no significant
373 trend over time (Fig. 3h). In addition, $\delta^{15}N$-PN increased from 14.8 ±0.3 to 3078 ±180 ‰
374 and from 15.0 ±0.5 to 2738 ±66 ‰ for 80% and 2% sPAR sample, respectively (Fig.
375 3i). These significant changes in both concentration and isotopic compositions of
376 nitrogen pools over time suggested that nitrogen transformed significantly among
377 pools and the labelled ^{15}N in NH_4^+ flowed through the system except nitrate.

378 **3.3 Solutions of the matrix equation and STELLA extrapolation**

379 **3.3.1 Low nutrient case**

380 The matrix-derived rate constants (ki) and rates (Fi) are shown in Table 1(A) and
381 1(B), respectively. Under no remineralization condition (i.e. r_{NH4+} decreased 0% within
382 24 hours), the NO_x^- uptake (k4= 0.059 h^{-1}; F4 = 27.2 nmol L^{-1} h^{-1}) was the highest

among all in terms of flux, followed by NH_4^+ uptake (k1 = 0.038 h^{-1}; F1 = 4.9 nmol L^{-1} h^{-1}) and DON release (k5= 0.024 h^{-1}; F5 = 11.5 nmol L^{-1} h^{-1}). NH_4^+ uptake by bacteria (k6 = 0.007 h^{-1}; F6 = 1.0 nmol L^{-1} h^{-1}) was much lower than that by phytoplankton. The rate constant for nitrification (k3 = 0.0005 h^{-1}) was the lowest among all fluxes (F3 = 0.07 nmol L^{-1} h^{-1}).

By introducing initial ^{15}N and ^{14}N concentrations of NH_4^+, NO_x^-, PN and DON and the calculated rate constants (k1 to k6) into STELLA (Fig. S1), we obtained full time courses for all parameters (Fig. 4). Generally, the model outputs fitted well with the measured values except the last time point for PN associated ^{15}N concentration, $\delta^{15}N$, and r_N (Figs. 4 c, k and o). In general, the rates of the first time interval can well predict the following up observations, demonstrating a good predictive performance by using the matrix method instant rate. Since both substrates, e.g., ammonium and NO_x^-, fitted well within 24 hours, the extra non-fitted PN in observation after the time point of 12 hours likely indicated the participation of an additional nitrogen source, i.e., dissolved organic nitrogen that was utilized by phytoplankton (see discussion below) when inorganic nitrogen reached threshold levels (Sunda and Ransom, 2007).

In these test runs of regeneration with r_{NH4+} reduction by a total amount of 1 %, 10 %, 20 % and 50 %, we found that the NH_4^+ consumption rates (k1 and k6) increased as the regeneration (k2) increased (Table 1). As indicated in previous studies, such regeneration-induced isotope dilution indeed altered the original results (Table 1 and

Fig. 4). More specifically, greater NH_4^+ regeneration resulted in larger differences between these three PN-associated values (^{15}N-PN, δ^{15}N-PN, and r_{PN}) and the STELLA-projected data (Figs. 4 c, k and o). Meanwhile, the dilution effect was more significant after 12 hours of incubation. On the other hand, the effect of r_{NH4+} on NO_x^--associated parameters was trivial (Figs. 4 b, f, j, n and r). The comparison between the simulation and observation suggested that NH_4^+ regeneration needs to be considered for PN (i.e., uptake) when remineralization rate is high and incubation prolongs. Besides remineralization, offsets along the time course might possibly be induced by the community change as incubation prolongs.

3.3.2 High nutrient cases

The results of 80% sPAR and 2% sPAR under the assumption of fixed r_{NH4+} are shown in Table 2(A) and 2(B), respectively. For the high light sample (80 % sPAR), the NH_4^+ uptake by phytoplankton (F1, 397 nmol L^{-1} h^{-1}) and by bacteria (F8, 282 nmol L^{-1} h^{-1}) were much higher than the other rates and were followed by the NO_3^- uptake rate (F5, 149 nmol L^{-1} h^{-1}). The NO_2^- uptake (F3) rate was 29 nmol L^{-1} h^{-1}, much lower than that of NH_4^+ and NO_3^- uptake. The ammonia oxidation rate (F4) was 0.4 nmol L^{-1} h^{-1}, and the nitrite oxidation rate (F6) was zero (Table 2A). Since this incubation was conducted in winter with low temperature and under 80% sPAR light conditions, low rates of ammonium and nitrite oxidation were reasonable because both nitrifiers and NOB are sensitive to light (e.g. Olson, 1981a, 1981b; Horrigan et al., 1981; Ward, 2005;

423 Merbt et al., 2012; Smith et al., 2014). The DON release rate by phytoplankton (F7)
424 was zero in this case.
425 In comparison, all the rates in the condition of 2% sPAR showed a very similar
426 pattern (Table 2B). The only difference was that all the uptake rates were lower for the
427 2% sPAR except for ammonia oxidation, which was higher in the low light.
428 By introducing initial concentrations and calculated rate constants (k1–k8) into the
429 STELLA model (Fig. S2), we obtained successive variations of ^{15}N and ^{14}N
430 concentrations and r_N of NH_4^+, NO_2^-, NO_3^-, PN and DON over time (Fig. 5). In general,
431 the modeled and measured values remained consistent throughout the 15 h incubation,
432 demonstrating the capability of the isotope matrix method.
433 Similar to the low nutrient case, we evaluated the effect of regeneration (see Table
434 2 and Fig. 5A and 5B). Since ammonium uptake was the dominant process, the
435 alteration of the PN pool was more significant in comparison with the other pools (Figs.
436 5 d, n and s). We found again, as F2 increased, F1 and F8 increased to maintain a
437 constant reduction of the measured NH_4^+ concentration (Table 2). Similar to low
438 nutrient case, as regeneration increased the projected course of ^{15}N-PN deviated more
439 from observation and the turning point also appeared earlier, resulting in a larger
440 curvature of r-PN and $\delta^{15}N$-PN (Fig. 5d and 5s). This model exercise confirmed the
441 influence of the isotope dilution effect; however, the effect is insignificant in the early
442 stage of incubation.

4. Discussion

4.1 Method comparisons

4.1.1 Model structure and rate derivation

The most widespread ^{15}N model was proposed by Dugdale and Goering (1967), who assumed the isotopic and mass balances in the particulate fraction, resulting in the commonly used formula for nitrogenous nutrient uptake. Dugdale and Wilkerson (1986) modified their rate equations further and highlighted the importance of short-term incubation. Although short-term incubation was requested, Collos (1987) demonstrated that the formula based on the concentration of particles at the end of the experiment, rather than at the beginning, is more reliable when more than one N source are simultaneously incorporated by the phytoplankton population. That is, the equation by Collos (1987) corrected the bias caused by unlabeled multiple N utilization.

Different from the above mentioned equations, Blackburn (1979) and Caperon et al. (1979) proposed ^{15}N isotope dilution models based on the substrate rather than product. By measuring the isotope values and concentrations of the substrate, e.g. NH_4^+, and then both NH_4^+ consumptions (DON and/or PN as product) and regeneration rate can be obtained. Glibert et al. (1982) further modified the isotope dilution method and calculated the uptake rate into PN fraction by substituting the exponential average r_{NH4+} at the beginning and at the end of incubation to correct the isotope dilution existing in the model of Dugdale and Goering (1967). Besides method improvements, imbalance

463 was often observed between the substrate reduction and the increase in particulate
464 phase in field studies. Laws (1985) introduced a new model with consideration of the
465 imbalance and calculated the “net uptake rate” (into PN). Later on, Bronk and Glibert
466 (1991) revised Law’s model on the basis of the model proposed by Glibert et al. (1982)
467 to calculate the “gross uptake rate” (substrate incorporation into PON plus DON).
468 Overall speaking, none of the above models considered mass balance at whole system
469 scale. Although rates were obtained via analytical solutions, the bias potential due to
470 multiple flows was not completely solved.

471 To solve multiple co-occurring N processes, Elskens et al. (2002) formulated a
472 new model, containing 3n+1 equations (n stands for the number of labelled N
473 substrate) and 3n+1 flux rates, by taking multiple co-occurring N fluxes in natural
474 system into account. Approximate rates in their model were resolved by a weighted
475 least squares technique. Additionally, Elskens et al. (2005) created a process-oriented
476 model (PROM) accounting for as many N processes as needed to quantify how
477 specific underlying assumptions affect the estimation behavior of all above-mentioned
478 models. The authors concluded uncertainties may increase as the incubation prolongs
479 and oversimplified models may risk bias when their underlying assumptions are
480 violated. The most recent attempt to resolve simultaneous N processes was conducted
481 by Pfister et al. (2016) who applied parallel incubations (^{15}N labelled NH_4^+ and NO_3^-)
482 in tidepools to measure multiple flows among benthic, ammonium, nitrite and nitrate

483 pools. In their experiment, six differential equations (with seven unknowns) were
484 constructed basing on mass and isotope balances and solved by using the ODE
485 function of R language. Since benthic algae were not measured due to difficulty in
486 sampling and spatial heterogeneity in biomass, the whole system scale mass balance
487 cannot be reached; thus, the flux of DON release cannot be obtained.

488 Compared with methods or models mentioned above, the advantages of isotope
489 matrix method include (1) the potential biases caused by multi-flows were considered
490 under the circumstance of mass balance at system scale; (2) one tracer addition for
491 multiple *in situ* flows (parallel incubations, i.e., dark and light or $^{15}NH_4^+$ and $^{15}NO_x^-$,
492 were not needed); (3) simple post-hoc data processing and unique solution can be
493 obtained via matrix derivation; (4) no extra laboratory work is demanded (see below).

494 **4.1.2 Rate comparisons**

495 Following Pfister et al. (2016), we estimated all N transformation rates via ODE
496 for the three cases on the assumption that there is no remineralization for comparison
497 (see Table 1−3). In general, the rate values obtained by the matrix and ODE were
498 consistent. The rate difference, if any, was caused by the duration for integration, i.e.,
499 shorter time (the first two time points for calculation) for isotope matrix method and
500 longer time (4 or 5 points for the entire incubation) for ODE. In Pfister et al. (2016), 3
501 monitoring points within 5 hours were implemented for ODE. Unfortunately, such
502 intensive sampling for on-deck incubation is not practical; however, we still strongly

recommend the short-term incubation for water column study as previously suggested. With proper duration, two time points for integration may be more convenient and realistic for instant rate measure.

Below, we present a comparison with conventional source-product rate measurements (Collos, 1987) of ammonium oxidation and uptake (Table 3). The matrix-derived NH_4^+ uptake rates for all experimental cases were consistent with those (difference < 8%) from the traditional source-product method when the final PN concentration was applied for calculation. The deviations were larger (13−21%) when the initial PN was applied, which was supported by the conclusion of previous studies that estimate involving the final PN concentration more reliable. Obviously, deviation could be higher when the phytoplankton growth rate was higher.

On the other hand, the end-products of ammonium oxidation or nitrification are consumed by phytoplankton continuously, particularly in euphotic layer full of photosynthetic autotrophs. In many cases, nitrate uptake occurs in both light and dark conditions (e.g. Dugdale and Goering, 1967; Lipschultz, 2002; Mulholland and Lomas, 2008). The significant consumption of end-products (NO_x^- and NO_2^-) apparently violate the underlying assumption of source-product rate calculation. Therefore, the NH_4^+ oxidation/nitrification rate could not be obtained, such as all cases in our study since phytoplankton consumption resulted in a net reduction of NO_x^- (Figs. 2b, 3b and 3c) (see Table 3).

In most cases, the final isotopic composition rather than final concentration of NO_x^- was measured; as such, researchers may not be aware of the greater $^{15}NO_x^-$ outflow than inflow. For dark incubation, researchers may also assume insignificant NO_x^- consumption. However, the "net decrease in end-product" is almost unavoidable when incubation is conducted under simulated *in situ* light condition for ammonium oxidation. To overcome this consumption effect induced by the first-order reaction, Santoro et al. (2010, 2013) took NO_x^- removal into account and formulated a new equation, a function of nitrification rate (F) and NO_x^- uptake rate (k). Following Santoro et al. (2010), we calculated the nitrification rate for the low-nutrient case (via a nonlinear least-squares curve-fitting routine in Matlab by using the first three time points of the ^{15}N-NO_x^- /^{14}N- NO_x^-measurements) to be 0.05 nmol L^{-1} h^{-1} (Table 3), which was (~30%) lower than the matrix-derived rate (0.07 nmol L^{-1} h^{-1}). By contrast, their nitrate uptake rate (k = 0.010 h^{-1}) was only one-sixth of that (0.059 h^{-1}) derived from the matrix method, although a comparable nitrification rate was obtained when the consumption term was taken into account.

Surprisingly, when we introduced the two parameters by using the method of Santoro et al. (2010) into STELLA to generate the time courses of parameters, we found simulations of $\delta^{15}NO_x^-$ and r_{NOx-} agreed well with that of isotope matrix method (Figs. 4j and 4n), yet, much slower decreasing trends were found for $^{15}NO_x^-$, $^{14}NO_x^-$, and NO_x^- (Figs. 4 b, f and r). Finally, we realized that the formula produced by

543 Santoro et al. (2010) is constrained only by the ratio changes rather than the individual
544 concentration changes in $^{15}NO_x^-$ and $^{14}NO_x^-$. Thus, the nonlinear curve-fitting method
545 by Matlab may only provide a correct simulation for the ratio change. This implies that
546 the nitrate uptake rate derived from the non-linear curve-fitting method in Matlab
547 should be validated also by the final concentration of nitrate, as was done by Santoro et
548 al. (2013).

549 In summary, (1) an accurate measurement of concentration time series is vital for
550 all kinds of transformation rate estimate including the isotope matrix method and (2)
551 the isotope matrix method overcame various biases that traditional methods might
552 encounter.

553 **4.2 Implications for nitrogen biogeochemical processes**

554 Through the isotope matrix method, biogeochemical implications were obtained
555 from various aspects.

556 **4.2.1 Remineralization, regeneration and community succession**

557 The matrix solution fit well with the model runs with variable r-NH_4^+ in early
558 stage, suggesting that dilution effect was negligible during the early incubation period
559 at least in our case. Dilution effect could be significant when remineralization is
560 intensive and incubation prolongs. Pfister et al. (2016) found macrofauna (mussel)
561 play an important role in remineralization. While zooplankton in the water column of

562 our sampled cases was not abundant, it might be a reason for low remineralization
563 rates in our short-term incubation.
564 In the WNP low nutrient case, after 24-hour incubation the levels of nitrate and
565 ammonium approached the concentration threshold for phytoplankton utilization (e.g.,
566 <30−40 nM NH_4^+ for *Emiliania huxleyi*; Sunda and Ransom, 2007). In Figure 4,
567 STELLA projection fitted well with PN parameters only for the first 12 hours. In this
568 case, in fact, we have observed phytoplankton succession. Our flow cytometry data
569 (shown in authors reply for Reviewer #2) demonstrated that the cell number of living
570 eukaryotes (4 times higher than *Synechococcus*) increased in the first 24 hours and
571 started to drop rapidly after 24 hours. On the contrary, the growth of *Synechococcus*
572 continued throughout 94 hours under constantly low nitrogen nutrient situation. Such
573 phenomenon suggested that phytoplankton community competed for nitrogen source
574 and a major community shift started at around 24 hours. After the time point of 12
575 hours, observed parameters associated with PN was higher than the projection by
576 STELLA. The most intriguing phenomenon among PN associated parameters was the
577 additional ^{15}N, which should not come from $^{15}NH_4^+$, in PN. The most likely nitrogen
578 source candidate with enriched ^{15}N to support *Synechococcus* growth was the nitrogen
579 released from dead eukaryotes, which contained freshly consumed ^{15}N tracer, rather
580 than the ambient DON. More studies are needed to explore nutrient thresholds for

different phytoplankton species. Nevertheless, our results suggested that short-term incubation is crucial for nitrogen uptake studies in oligotrophic ocean.

4.2.2 Evaluate the contribution of nitrification to new production

Nitrification in the sunlit ocean drew not much attention until recent decades after the widespread ammonia oxidizing archaea (AOA) discovery in the perspective of molecular evidence (Francis et al., 2005; Santoro et al., 2010, 2013; Smith et al., 2014) and rate measurements based on isotope (Ward, 2011; Santoro et al., 2010; Grundle et al., 2013; Smith et al., 2014). As mentioned in Introduction, the conventional "new" production has been overestimated 19−33% on a global scale due to the "regenerated" nitrate via nitrification process. However, a more realistic evaluation for the fractional contribution of nitrification to NO_3^- uptake can only be achieved when the incubation is conducted in the same bottle under *in situ* light conditions instead of parallel incubations in dark and light. The isotope matrix method is so far the most convenient and suitable method for evaluating the relative importance of co-occuring nitrification and new production in the euphotic ocean. In all our experimental cases, the contributions of nitrification to new production were < 1% (Table 4). The relatively low contribution was probably due to the light inhibition on nitrifiers for the WNP case and because of the low temperature in the sampling season.

Nevertheless, light effect in our case studies is significant. Light suppresses nitrification (Ward, 2005; Merbt et al., 2012; Peng et al., 2016). NH_4^+ oxidation rate in

601 80% sPAR reduced by 36% relative to that in 2% sPAR. Results agreed with current
602 knowledge although some recent evidences showed that some taxa of marine AOA
603 hold genetic capabilities to reduce oxidative stress and to repair ultraviolet damage
604 (Luo et al., 2014; Santoro et al., 2015). More study cases are needed in the future to
605 explore vertical distributions of the relative contribution of nitrification to new
606 production in euphotic zone.

607 **4.2.3 Nutrient preference**

608 Phytoplankton takes different nitrogenous species as nutrients for growth.
609 McCarthy et al. (1977) introduced a relative preference index (PRI) to assess the
610 relative utilization of a specific N form, and when RPI value >1 indicates a preference
611 for the specific substrate over the other N forms. As shown in Table 4, in the NO_3^-
612 prevailed low nutrient case, the PRI (NO_3^-) was very close but slightly higher to PRI
613 (NH_4^+), which was probably due to the phytoplankton community structure as
614 mentioned above. This result was in line with the result in the Sargasso Sea (Fawcett et
615 al., 2011). While in the high NH_4^+ bay, the PRI (NH_4^+) > 1 > PRI (NO_3^-) > PRI (NO_2^-),
616 suggesting that phytoplankton preferred NH_4^+ over NO_3^- and NO_2^-, similar to the result
617 in Chesapeake Bay (McCarthy et al., 1977).

618 **4.2.4 Quantify various ammonium consumption pathways**

In the upper ocean, NH_4^+ cycles rapidly due to various microorganisms's metabolic pathways competing for ammonium. Ammonium may serve as nitrogen source for phytoplankton assimilation, and as energy source for ammonia oxidizing organisms (AOM). Moreover, many studies have shown that bacteria also play a part in NH_4^+ utilization (Middelburg and Nieuwenhuize, 2000; Veuger et al., 2004). Our result in the low nutrient case showed that phytoplankton was the main NH_4^+ consumer (82% of the total NH_4^+ consumption), bacteria accounted for another ~17% and AOM utilized the rest 1%. While in the eutrophic WYW bay, phytoplankton and bacteria each consumed ~50% of the total NH_4^+ (Table 4).

5. Conclusion

This isotope matrix method was designed specifically for euphotic water column incubation under simulated *in situ* condition. By considering multi-flows among pools on the assumption of mass balance at the whole system level, we minimized potential biases caused by non-targeted processes in traditional source-product methods. Given the progress in analytical techniques for concentration and isotopic composition of nitrogen species, the isotope matrix method presents a promising avenue for the study of rates of nitrogen processes with a system-wide perspective. Furthermore, the matrix method is also appropriate for probing the effects of environmental factors (e.g., CO_2, pH, temperature, and light intensity) on the interactive N processes in one single incubation bottle.

Acknowledgement

We sincerely thank Wenbin Zou and Tao Huang at the State Key Laboratory of Marine Environmental Science (Xiamen University, China) for their valuable help with the water sampling and the on-board trace NH_4^+ concentration analysis during the 2015 NWP cruise. Yu-ting Shih from the Department of Geology at National Taiwan University in Taiwan is thanked for his help on ODE application. This research was funded by the National Natural Science Foundation of China (NSFC U1305233, 2014CB953702, 91328207, 2015CB954003).

References

Beman, J. M., Popp, B. N., and Alford, S. E.: Quantification of ammonia oxidation rates and ammonia-oxidizing archaea and bacteria at high resolution in the Gulf of California and eastern tropical North Pacific Ocean, Limnol. Oceanogr., 57, 711-726, doi:10.4319/lo.2012.57.3.0711, 2012.

Blackburn, T. H.: Method for Measuring Rates of NH_4^+ Turnover in Anoxic Marine Sediments, Using a ^{15}N-NH_4^+ Dilution Technique, Appl. Environ. Microbiol., 37, 760-765, 1979.

Braman, R. S., and Hendrix, S. A.: Nanogram nitrite and nitrate determination in environmental and biological materials by vanadium (III) reduction with chemiluminescence detection, Anal. Chem., 61, 2715-2718, doi: 10.1021/ac00199a007, 1989.

Brauwere, A. D., Ridder, F. D., Pintelon, R., Elskens, M., Schoukens, J., and Baeyens, W.: Model selection through a statistical analysis of the minimum of a weighted least squares cost function, Chemom. Intell. Lab. Syst., 76, 163-173, doi:10.1016/j.chemolab.2004.10.006, 2005.

Bronk, D., Killberg-Thoreson, L., Sipler, R., Mulholland, M., Roberts, Q., Bernhardt, P., Garrett, M., O'Neil, J., and Heil, C.: Nitrogen uptake and regeneration (ammonium regeneration, nitrification and photoproduction) in waters of the West Florida Shelf

prone to blooms of Karenia brevis, Harmful Algae, 38, 50-62, doi:10.1016/j.hal.2014.04.007, 2014.

Bronk, D. A., and Glibert, P. M.: A ^{15}N tracer method for the measurement of dissolved organic nitrogen release by phytoplankton. Mar. Ecol. Prog. Ser., Marine Ecology Progress, 77, 1991.

Bronk, D. A., Glibert, P. M., and Ward, B. B.: Nitrogen uptake, dissolved organic nitrogen release, and new production, Science, 265, 1843-1846, 1994.

Bronk, D. A., and Ward, B. B.: Magnitude of dissolved organic nitrogen release relative to gross nitrogen uptake in marine systems, Limnol. Oceanogr., 45, 1879-1883, doi: 10.4319/lo.2000.45.8.1879, 2000.

Caperon, J., Schell, D., Hirota, J., and Laws, E.: Ammonium excretion rates in Kaneohe Bay, Hawaii, measured by a ^{15}N isotope dilution technique, Mar. Biol., 54, 33-40, doi: 10.1007/BF00387049, 1979.

Casciotti, K., Sigman, D., Hastings, M. G., Böhlke, J., and Hilkert, A.: Measurement of the oxygen isotopic composition of nitrate in seawater and freshwater using the denitrifier method, Anal. Chem., 74, 4905-4912, 2002.

Casciotti, K. L.: Nitrogen and Oxygen Isotopic Studies of the Marine Nitrogen Cycle, Ann. Rev. Mar. Sci., 8, 379-407, doi: 10.1146/annurev-marine-010213-135052, 2016.

Chen, Y.-l. L.: Spatial and seasonal variations of nitrate-based new production and primary production in the South China Sea, Deep Sea Res. Part I Oceanogr. Res. Pap., 52, 319-340, doi:10.1016/j.dsr.2004.11.001, 2005.

Collos, Y.: Calculations of ^{15}N uptake rates by phytoplankton assimilating one or several nitrogen sources, International Journal of Radiation Applications and Instrumentation. Part A. Applied Radiation and Isotopes, 38, 275-282, doi:10.1016/0883-2889(87)90038-4, 1987.

Daims, H., Lebedeva, E. V., Pjevac, P., Han, P., Herbold, C., Albertsen, M., Jehmlich, N., Palatinszky, M., Vierheilig, J., Bulaev, A., Kirkegaard, R. H., von Bergen, M., Rattei, T., Bendinger, B., Nielsen, P. H., and Wagner, M.: Complete nitrification by Nitrospira bacteria, Nature, 528, 504-509, 10.1038/nature16461, doi:10.1038/nature16461, 2015.

Dugdale, R., and Goering, J.: Uptake of new and regenerated forms of nitrogen in primary productivity, Limnol. Oceanogr., 12, 196-206, doi: 10.4319/lo.1967.12.2.0196, 1967.

699 Dugdale, R., and Wilkerson, F.: The use of ^{15}N to measure nitrogen uptake in eutrophic
700 oceans; experimental considerations, Limnol. Oceanogr., 31, 673-689, doi:
701 10.4319/lo.1986.31.4.0673, 1986.

702 Elskens, M., Baeyens, W., Cattaldo, T., Dehairs, F., and Griffiths, B.: N uptake
703 conditions during summer in the Subantarctic and Polar Frontal Zones of the Australian
704 sector of the Southern Ocean, J. Geophys. Res.: Oceans, 107, 3-1-3-11,
705 doi:10.1029/2001JC000897, 2002.

706 Elskens, M., Baeyens, W., Brion, N., Galan, S. D., Goeyens, L., and Brauwere, A. D.:
707 Reliability of N flux rates estimated from ^{15}N enrichment and dilution experiments in
708 aquatic systems, Global Biogeochem. Cycles, 19, 573-574,
709 doi:10.1029/2004GB002332, 2005.

710 Falkowski, P. G.: Evolution of the nitrogen cycle and its influence on the biological
711 sequestration of CO_2 in the ocean, Nature, 387, 272-275, doi: 10.1038/387272a0, 1997.

712 Fawcett, S. E., Lomas, M. W., Casey, J. R., Ward, B. B., and Sigman, D. M.:
713 Assimilation of upwelled nitrate by small eukaryotes in the Sargasso Sea, Nature
714 Geoscience, 4, 717-722, doi:10.1038/ngeo1265, 2011.

715 Francis, C. A., Roberts, K. J., Beman, J. M., Santoro, A. E., and Oakley, B. B.: Ubiquity
716 and diversity of ammonia-oxidizing archaea in water columns and sediments of the
717 ocean, Proceedings of the National Academy of Sciences, 102, 14683-14688, doi:
718 10.1073/pnas.0506625102, 2005.

719 Gilbert, P. M., Lipschultz, F., McCarthy, J. J., and Altabet, M. A.: Isotope dilution
720 models of uptake and remineralization of ammonium by marine plankton, Limnol.
721 Oceanogr., 27, 639-650, 1982.

722 Granger, J., and Sigman, D. M.: Removal of nitrite with sulfamic acid for nitrate N and
723 O isotope analysis with the denitrifier method, Rapid Commun. Mass Spectrom., 23,
724 3753-3762, 10.1002/rcm.4307, doi: 10.1002/rcm.4307, 2009.

725 Grundle, D. S., Juniper, S. K., and Giesbrecht, K. E.: Euphotic zone nitrification in the
726 NE subarctic Pacific: Implications for measurements of new production, Mar. Chem.,
727 155, 113-123, doi:10.1016/j.marchem.2013.06.004, 2013.

728 Hannon, J. E., and Böhlke, J. K.: Determination of the delta ($^{15}N/^{14}N$) of Ammonium
729 (NH_4^+) in Water: RSIL Lab Code 2898, US Geological Survey 2328-7055, 2008.

730 Harrison, P. J., and Davis, C. O.: Use of the perturbation technique to measure nutrient
731 uptake rates of natural phytoplankton populations, Deep Sea Res., 24, 247-255,
732 doi:10.1016/S0146-6291(77)80003-9, 1977.

733 Harvey, W. A., and Caperon, J.: The rate of utilization of urea, ammonium, and nitrate
734 by natural populations of marine phytoplankton in a eutrophic environment, Pacific
735 Science, 30 (4), 329-340, http://hdl.handle.net/10125/1169, 1976.

736 Holmes, R., McClelland, J., Sigman, D., Fry, B., and Peterson, B.: Measuring ^{15}N–
737 NH_4^+ in marine, estuarine and fresh waters: An adaptation of the ammonia diffusion
738 method for samples with low ammonium concentrations, Mar. Chem., 60, 235-243,
739 doi:10.1016/S0304-4203(97)00099-6, 1998.

740 Horrigan, S., Carlucci, A., and Williams, P.: Light inhibition of nitrification in
741 sea-surface films [California], J. Mar. Res., 1981.

742 Howard, M. D. A., Cochlan, W. P., Ladizinsky, N., and Kudela, R. M.: Nitrogenous
743 preference of toxigenic Pseudo-nitzschia australis (Bacillariophyceae) from field and
744 laboratory experiments, Harmful Algae, 6, 206-217, doi:10.1016/j.hal.2006.06.003,
745 2007.

746 Hsiao, S.-Y., Hsu, T.-C., Liu, J.-w., Xie, X., Zhang, Y., Lin, J., Wang, H., Yang, J.-Y.,
747 Hsu, S.-C., and Dai, M.: Nitrification and its oxygen consumption along the turbid
748 Chang Jiang River plume, Biogeosciences, 11, 2083-2098,
749 doi:10.5194/bg-11-2083-2014, 2014.

750 Knapp, A. N., Sigman, D. M., and Lipschultz, F.: N isotopic composition of dissolved
751 organic nitrogen and nitrate at the Bermuda Atlantic Time-series Study site, Global
752 Biogeochem. Cycles, 19, doi: 10.1029/2004GB002320, 2005.

753 Koroleff, F.: Simultaneous oxidation of nitrogen and phosphorus compounds by
754 persulfate, Methods of seawater analysis, 2, 205-206, 1983.

755 Laws, E. A.: Analytic Models of NH_4^+ Uptake and Regeneration Experiments, Limnol.
756 Oceanogr., 30, 1340–1350, 1985.

757 Lipschultz, F.: A time-series assessment of the nitrogen cycle at BATS, Deep Sea Res.
758 Part II Top. Stud. Oceanogr., 48, 1897-1924, doi:10.1016/S0967-0645(00)00168-5,
759 2001.

760 Lipschultz, F.: Isotope Tracer Methods for Studies of the Marine Nitrogen Cycle, in
761 Nitrogen in the marine environment, edited by: Capone, D. A., Bronk, D. A.,
762 Mulholland, M. R., Carpenter, E. J., Academic Press, London, U.K., 303-384, 2008.

763 Lomas, M. W., and Lipschultz, F.: Forming the primary nitrite maximum: Nitrifiers or
764 phytoplankton?, Limnol. Oceanogr., 51, 2453-2467, doi: 10.4319/lo.2006.51.5.2453,
765 2006.

766 Luo, H., Tolar, B. B., Swan, B. K., Zhang, C. L., Stepanauskas, R., Ann, M. M., and
767 Hollibaugh, J. T.: Single-cell genomics shedding light on marine Thaumarchaeota
768 diversification, ISME Journal, 8, 732-736, doi:10.1038/ismej.2013.202, 2014.

769 Marchant, H. K., Mohr, W., Kuypers, M. M. M.: Recent advances in marine N-cycle
770 studies using ^{15}N labeling methods. Curr. Opin. Biotechnol., 41, 53-59,
771 doi:10.1016/j.copbio.2016.04.019, 2016.

772 McCarthy, J. J., and Eppley, R. W.: A comparison of chemical, isotopic, and enzymatic
773 methods for measuring nitrogen assimilation of marine phytoplankton, Limnol.
774 Oceanogr., 17, 371-382, doi: 10.4319/lo.1972.17.3.0371, 1972.

775 Mccarthy, J. J., Taylor, and Taft, J. L.: Nitrogenous nutrition of the plankton in the
776 Chesapeake Bay.1. Nutrient availability and phytoplankton preferences, Limnol.
777 Oceanogr., 22, 996-1011, 1977.

778 McIlvin, M. R., and Altabet, M. A.: Chemical conversion of nitrate and nitrite to nitrous
779 oxide for nitrogen and oxygen isotopic analysis in freshwater and seawater, Anal.
780 Chem., 77, 5589-5595, doi: 10.1021/ac050528s, 2005.

781 Merbt, S. N., Stahl, D. A., Casamayor, E. O., Mart ́ı E., Nicol, G. W., and Prosser, J. I.:
782 Differential photoinhibition of bacterial and archaeal ammonia oxidation, FEMS
783 Microbiol. Lett., 327, 41-46, doi: http://dx.doi.org/10.1111/j.1574-6968.2011.02457.x,
784 2012.

785 Middelburg, J. J., and Nieuwenhuize, J.: Uptake of dissolved inorganic nitrogen in
786 turbid, tidal estuaries, Mar. Ecol. Prog. Ser., 192, 79-88, doi:10.3354/meps192079,
787 2000.

788 Mulholland, M. R., and Lomas, M. W.: Nitrogen uptake and assimilation, in Nitrogen
789 in the marine environment, edited by: Capone, D. A., Bronk, D. A., Mulholland, M. R.,
790 Carpenter, E. J., Academic Press, London, U.K., 303-384, 2008.

791 Newell, S. E., Fawcett, S. E., and Ward, B. B.: Depth distribution of ammonia oxidation
792 rates and ammonia-oxidizer community composition in the Sargasso Sea, Limnol.
793 Oceanogr., 58, 1491-1500, doi:10.4319/lo.2013.58.4.1491, 2013.

794 Olson, R.: ^{15}N tracer studies of the primary nitrite maximum, J. Mar. Res., 39, 203-226,
795 1981a.

796 Olson, R. J.: Differential photoinhibition of marine nitrifying bacteria: a possible
797 mechanism for the formation of the primary nitrite maximum, J. Mar. Res., 39, 227-238,
798 1981b.

799 Painter, S. C., Patey, M. D., Tarran, G. A., and Torres-Valdés, S.: Picoeukaryote
800 distribution in relation to nitrate uptake in the oceanic nitracline, Aquat. Microb. Ecol.,
801 72, 195-213, doi:10.3354/ame01695, 2014.

802 Pakulski, J., Benner, R., Amon, R., Eadie, B., and Whitledge, T.: Community
803 metabolism and nutrient cycling in the Mississippi River plume: evidence for intense
804 nitrification at intermediate salinities, Mar. Ecol. Prog. Ser., 117, 207, 1995.

805 Peng, X., Fuchsman, C. A., Jayakumar, A., Warner, M. J., Devol, A. H., and Ward, B.
806 B.: Revisiting nitrification in the eastern tropical South Pacific: A focus on controls, J.
807 Geophys. Res.: Oceans, doi: 10.1002/2015JC011455, 2016.

808 Pfister, C. A., Altabet, M. A., Pather, S., and Dwyer, G.: Tracer experiment and model
809 evidence for macrofaunal shaping of microbial nitrogen functions along rocky shores,
810 Biogeosciences, 13, 3519-3531, doi:10.5194/bg-13-3519-2016, 2016.

811 Raimbault, P., and Garcia, N.: Evidence for efficient regenerated production and
812 dinitrogen fixation in nitrogen-deficient waters of the South Pacific Ocean: impact on
813 new and export production estimates, Biogeosciences, 5, 323-338, 2008.

814 Santoro, A., Sakamoto, C., Smith, J., Plant, J., Gehman, A., Worden, A., Johnson, K.,
815 Francis, C., and Casciotti, K.: Measurements of nitrite production in and around the
816 primary nitrite maximum in the central California Current, Biogeosciences, 10,
817 7395-7410, doi:10.5194/bg-10-7395-2013, 2013.

818 Santoro, A. E., Casciotti, K. L., and Francis, C. A.: Activity, abundance and diversity of
819 nitrifying archaea and bacteria in the central California Current, Environ. Microbiol.,
820 12, 1989-2006, doi. L., and Francis, C. A.: Activity, abundance and diversity of
821 nitrifying archaea and bacteria in the central California Current, Environ. Microbiol.,
822 12, 1989-2006, 2010.

823 Santoro, A. E., Dupont, C. L., Richter, R. A., Craig, M. T., Carini, P., Mcilvin, M. R.,
824 Yang, Y., Orsi, W. D., Moran, D. M., and Saito, M. A.: Genomic and proteomic
825 characterization of "Candidatus Nitrosopelagicus brevis": An ammonia-oxidizing
826 archaeon from the open ocean, Proceedings of the National Academy of Sciences of the
827 United States of America, 112, 1173-1178, doi: 10.1073/pnas.1416223112, 2015.

828 Sigman, D., Casciotti, K., Andreani, M., Barford, C., Galanter, M., and Böhlke, J.: A
829 bacterial method for the nitrogen isotopic analysis of nitrate in seawater and freshwater,
830 Anal. Chem., 73, 4145-4153, doi: 10.1021/ac010088e, 2001.

831 Smith, J. M., Chavez, F. P., and Francis, C. A.: Ammonium uptake by phytoplankton
832 regulates nitrification in the sunlit ocean, PloS One, 9, e108173, doi:
833 org/10.1371/journal.pone.0108173, 2014.

834 Sunda, W. G., and Ransom, H. D.: Ammonium uptake and growth limitation in marine
835 phytoplankton, Limnol. Oceanogr., 52, 2496–2506, 2007.

836 van Kessel, M. A., Speth, D. R., Albertsen, M., Nielsen, P. H., Opden Camp, H. J.,
837 Kartal, B., Jetten, M. S., and Lucker, S.: Complete nitrification by a single
838 microorganism, Nature, 528, 555-559, 10.1038/nature16459, doi:10.1038/nature16459,
839 2015.

840 Varela, M. M., Bode, A., Fernandez, E., Gonzalez, N., Kitidis, V., Varela, M., and
841 Woodward, E.: Nitrogen uptake and dissolved organic nitrogen release in planktonic
842 communities characterised by phytoplankton size–structure in the Central Atlantic
843 Ocean, Deep Sea Res. Part I Oceanogr. Res. Pap., 52, 1637-1661,
844 doi:10.1016/j.dsr.2005.03.005, 2005.

845 Veuger, B., Middelburg, J. J., Boschker, H. T. S., Nieuwenhuize, J., Rijswijk, P. V.,
846 Rochelle-Newall, E. J., and Navarro, N.: Microbial uptake of dissolved organic and
847 inorganic nitrogen in Randers Fjord, Estuarine Coastal and Shelf Science, 61, 507–515,
848 doi:10.1016/j.ecss.2004.06.014, 2004.

849 Wada, E., and Hatton, A.: Nitrite metabolism in the euphotic layer of the central North
850 Pacific Ocean, Limnol. Oceanogr., 16, 766-772, doi: 10.4319/lo.1971.16.5.0766 1971.

851 Ward, B. B.: Temporal variability in nitrification rates and related biogeochemical
852 factors in Monterey Bay, California, USA, Mar. Ecol. Prog. Ser., 292, 109,
853 doi:10.3354/meps292097, 2005.

854 Ward, B. B.: Nitrification in marine systems, in Nitrogen in the marine environment,
855 edited by: Capone, D. A., Bronk, D. A., Mulholland, M. R., Carpenter, E. J., Academic
856 Press, London, U.K., 5, 199-261, 2008.

857 Ward, B. B.: Measurement and distribution of nitrification rates in the oceans, in
858 Methods in enzymology, edited by Abelson, J. N., Simon, M. I., Academic Press,
859 London, U.K., 486, 307-323, 2011.

860 Yool, A., Martin, A. P., Fernández, C., and Clark, D. R.: The significance of
861 nitrification for oceanic new production, Nature, 447, 999-1002,
862 doi:10.1038/nature05885, 2007.

863 Zehr, J. P., and Kudela, R. M.: Nitrogen cycle of the open ocean: from genes to
864 ecosystems, Ann. Rev. Mar. Sci., 3, 197-225, doi:
865 10.1146/annurev-marine-120709-142819, 2011.

866 Zhang, L., Altabet, M. A., Wu, T., and Hadas, O.: Sensitive measurement of NH_4^+
867 $^{15}N/^{14}N$ ($\delta^{15}NH_4^+$) at natural abundance levels in fresh and saltwaters, Anal. Chem., 79,
868 5297-5303, doi: 10.1021/ac070106d, 2007.

869 Zhu, Y., Yuan, D., Huang, Y., Ma, J., and Feng, S.: A sensitive flow-batch system for
870 on board determination of ultra-trace ammonium in seawater: Method development and
871 shipboard application, Anal. Chim. Acta., 794, 47-54, 10.1016/j.aca.2013.08.009,
872 doi:10.1016/j.aca.2013.08.009, 2013.

873

Table 1. The isotope matrix results for (A) the specific rates and (B) average rates of N processes in the low-nutrient case during the first interval under different r_{NH4+} variation conditions. And all N transformation rates via ODE following Pfister et al. (2016) on the assumption of no remineralization were estimated for comparison. Note r_{NH4+} variation was manipulated artificially by decreasing r_{NH4+} values at a constant reduction rate and the total reduction of rNH4+ was 0%, 1%, 10%, 20% and 50% of the full time span (24 h) of incubation.

(A)

Rate constant (k) h^{-1}	The percentage of r_{NH4+} decrease in 24 h					
	0		1%	10%	20%	50%
	ODE	Isotope Matrix				
NH_4^+ uptake (k1)	0.040	0.038	0.038	0.038	0.038	0.039
Remineralization (k2)	0	0	0.00001	0.0001	0.0002	0.001
NH_4^+ oxidation (k3)	0.0004	0.0005	0.0005	0.0005	0.0005	0.0005
NO_x^- uptake (k4)	0.060	0.059	0.059	0.059	0.059	0.059
DON release (k5)	0.017	0.024	0.024	0.024	0.024	0.024
Bacteria uptake NH_4^+ (k6)	0.005	0.007	0.008	0.011	0.015	0.028

(B)

Rate ($k \times$ C) nmol L^{-1} h^{-1}	The percentage of r_{NH4+} decrease in 24 h					
	0		1%	10%	20%	50%
	ODE	Isotope Matrix				
NH_4^+ uptake (F1)	3.8	4.9	4.9	4.9	5.0	5.1
Remineralization (F2)	0.0	0.0	0.1	0.6	1.2	3.0
NH_4^+ oxidation (F3)	0.04	0.07	0.1	0.1	0.1	0.7
NO_x^- uptake (F4)	19.3	27.2	27.2	27.2	27.2	27.2
DON release (F5)	9.6	11.5	11.5	11.6	11.6	11.8
Bacteria uptake NH_4^+ (F6)	0.5	1.0	1.0	1.5	2.0	3.7

Table 2. The isotope matrix results for the rates of N processes in the high-nutrient case at the depth of (A) 80% sPAR and (B) 2% sPAR under different r_{NH4+} variation conditions. And all N transformation rates via ODE following Pfister et al. (2016) on the assumption of no remineralization were estimated for comparison. Note: r_{NH4+} variation was manipulated artificially by decreasing r_{NH4+} values at a constant reduction rate and the total reduction of r_{NH4+} was 0%, 1%, 10%, 20% and 50% of the full time span (15 h) of incubation.

(A)

Rate (*k** C) nmol L^{-1} h^{-1}	The percentage of r_{NH4+} decrease in 15 h					
	0		1%	10%	20%	50%
	ODE	Isotope Matrix				
NH_4^+ uptake (F1)	360	397	397	399	401	408
Remineralization (F2)	0	0	21	211	424	1043
NO_2^- uptake (F3)	27	29	29	29	29	29
NH_4^+ oxidation (F4)	1.1	0.4	0.4	0.4	0.4	0.4
NO_3^- uptake (F5)	190	149	149	149	149	149
NO_2^- oxidation (F6)	1.7	0	0	0	0	0
DON release (F7)	0	0	0	0	0	0
Bacteria uptake NH_4^+ (F8)	268	282	303	490	701	1314

(B)

Rate (*k** C) nmol L^{-1} h^{-1}	The percentage of r_{NH4+} decrease in 15 h					
	0		1%	10%	20%	50%
	ODE	Isotope Matrix				
NH_4^+ uptake (F1)	228	208	208	209	211	216
Remineralization (F2)	0	0	18.1	179	361	895
NO_2^- uptake (F3)	7.3	3.1	3.1	3.1	3.1	3.1
NH_4^+ oxidation (F4)	1.1	0.7	0.7	0.7	0.7	0.7
NO_3^- uptake (F5)	106	72	72	72	72	72
NO_2^- oxidation (F6)	2.0	0	0	0	0	0
DON release (F7)	0	0	0	0	0	0
Bacteria uptake NH_4^+ (F8)	202	265	283	442	623	1152

892 **Table 3.** Comparison of the NH_4^+/ NO_x^- uptake and NH_4^+ oxidation/nitrification rates

893 derived from different methods.

Process	Case	Depth (m)	Isotope Matrix method (this study)	Rates based on Ref A*	Traditional method Ref B*	Rates followed Ref C*
			(nmol L^{-1} h^{-1})			
NH_4^+ uptake	Low nutrient	25	4.9	3.8	4.6	
Nitrification	Low nutrient	25	0.07	0.04	−	0.05
NO_x^- uptake	Low nutrient	25	27.2	19.3		4.6
NH_4^+ uptake	High -80%sPAR	0.2	397	360	387	
NH_4^+ oxidation	High -80%sPAR	0.2	0.4	1	−	
NH_4^+ uptake	High -2% sPAR	2.3	208	228	192	
NH_4^+ oxidation	High -2% sPAR	2.3	0.7	1	−	

894 Ref A* stands of rates calculation by ODE followed Pfister et al. (2016)

895 Ref B* stands of rates calculation followed Collos (1987)

896 Ref C* stands of rates calculation followed Santoro et al. (2010)

897

898 **Table 4.** The contribution of nitrification derived NO_x^- to NO_x^- uptake (%), N
899 preference index, and the proportion of NH_4^+ consumption by phytoplankton, bacteria
900 and nitrifier to total NH_4^+ consumption in low and high nutrient cases.

Case	Depth (m)	nitrification to NO_3^- uptake (%)	RPI for NH_4^+	RPI for NO_2^-	RPI for NO_3^-	*A/TNH_4^+ consumption (%)	*B/TNH_4^+ consumption (%)	*C/TNH_4^+ consumption (%)
Low nutrient	25	0.3	0.9		1.0	82.1	16.8	1.2
High -80%sPAR	0.2	0.3	1.6	0.6	0.5	58.4	41.5	0.1
High -2% sPAR	2.3	0.9	1.8	0.1	0.5	43.9	56.0	0.1

901 *A, *B, *C stands for NH_4^+ utilized by phytoplankton, bacteria and nitrifier,
902 respectively. TNH_4^+ consumption stands for total NH_4^+ consumption.

903

Figure Captions

Fig. 1. Model schemes with the most fundmental nitrogen transformation processes in low- (a) and high- (b) nutrient aquatic environments. Arrows stand for the transfer flux/rate from the reactant to product pool. The structure and inter-exchanges in the high-nutrient case (Fig. 1b) are the same as in (a), except that NO_x^- is divided into NO_2^- and NO_3^-.

Fig. 2. The observational data in the low-nutrient case for (a) [NH_4^+], (b) [NO_x^-], (c) [PN], (d) [TDN], (e) δ^{15}N-NO_x^-, (f) δ^{15}N-PN. The regular and inverse open triangles stand for the paralled samples and the analytical errors are shown.

Fig. 3. The observational data in the high-nutrient case for (a) [NH_4^+], (b) [NO_2^-], (c) [NO_3^-], (d) [PN], (e) [TDN], (f) [PN+TDN], (g) δ^{15}N-NO_2^-, (h) δ^{15}N-NO_3^- and (i) δ^{15}N-PN. The light and dark red diamonds stand for the paralled samples in 80% sPAR case and the black regular and inverse open triangles stand for the paralled samples in 2% sPAR case. The analytical errors are shown in figures.

Fig. 4. The observed and STELLA-derived values in the low-nutrient case for (a) [$^{15}NH_4^+$], (b) [$^{15}NO_x^-$], (c) [^{15}N-PN], (d) [^{15}N-DON], (e) [$^{14}NH_4^+$], (f) [$^{14}NO_x^-$], (g) [^{14}N-PN], (h) [^{14}N-DON], (i) r_{NH4+}, (j) r_{NOx-}, (k) r_{PN}, (l) r_{DON}, (m) δ^{15}N-NH_4^+, (n) δ^{15}N-NO_x^-, (o) δ^{15}N-PN, (p) δ^{15}N-DON, (q) [NH_4^+], (r) [NO_x^-], (s) [PN] and (t) [DON]. The black regular and inverse open triangles represent the paralleled observed values; the black, green, blue, magenta and pink solid lines stand for the STELLA model simulations when r_{NH4+} decreases 0%, 1%, 10%, 20% and 50% in 24 h, respectively. The dashed lines in (b), (f), (j), (n) and (r) were generated from nonlinear least-squares curve-fitting by Matlab following Santoro et al. (2010).

Fig. 5. The observed and STELLA-derived values in the high-nutrient case of (A) 80% sPAR depth and (B) 2% sPAR depth for (a) [$^{15}NH_4^+$], (b) [$^{15}NO_2^-$], (c) [$^{15}NO_3^-$], (d)

[^{15}N-PN], (e) [^{15}N-DON], (f) [$^{14}NH_4^+$], (g) [$^{14}NO_2^-$], (h) [$^{14}NO_3^-$], (i) [^{14}N-PN], (j) [^{14}N-DON], (k) r_{NH4+}, (l) r_{NO2-}, (m) r_{NO3-}, (n) r_{PN}, (o) r_{DON}, (p) $\delta^{15}N\text{-}NH_4^+$, (q) $\delta^{15}N\text{-}NO_2^-$, (r) $\delta^{15}N\text{-}NO_3^-$, (s) δ^{15}N-PN, (t) δ^{15}N-DON, (u) [NH_4^+], (v) [NO_2^-], (w) [NO_3^-] (x) [PN] and (y) [DON]. The black regular and inverse open triangles represent the duplicate observational values; the black, green, blue, magenta and pink solid lines represent the STELLA model simulations of r_{NH4+} decreases 0%, 1%, 10%, 20% and 50% in 15 h, respectively.

937 **Fig. 1**

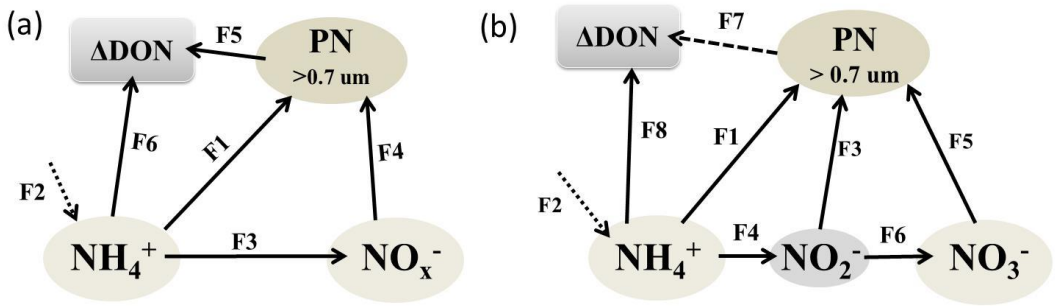

938

939

940 **Fig. 2**

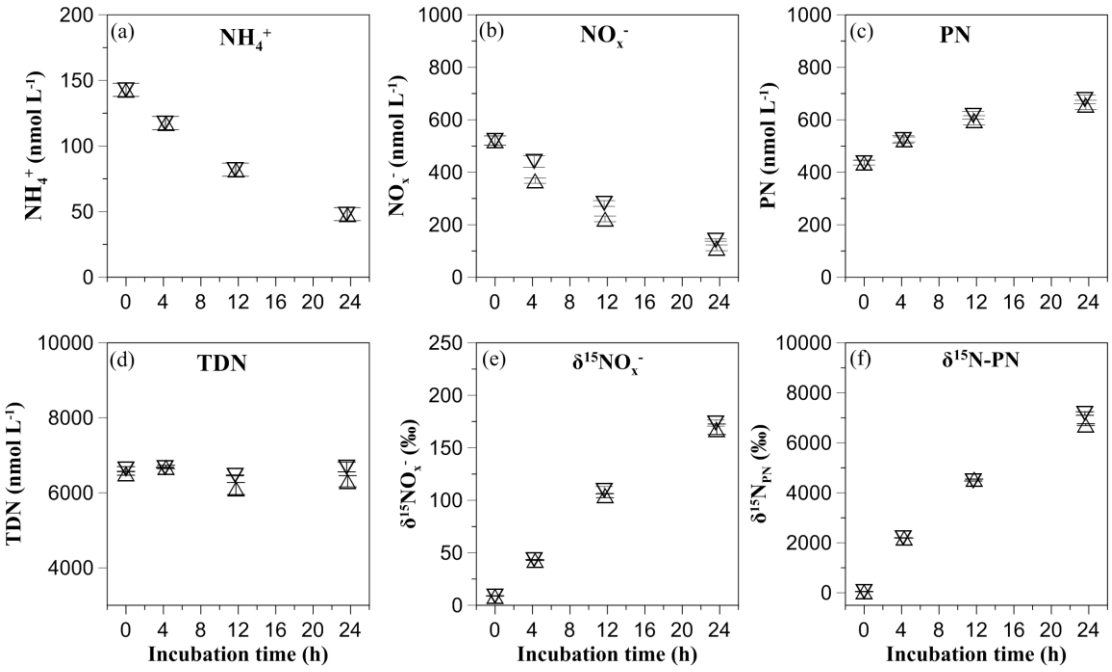

941

942

943 **Fig. 3**

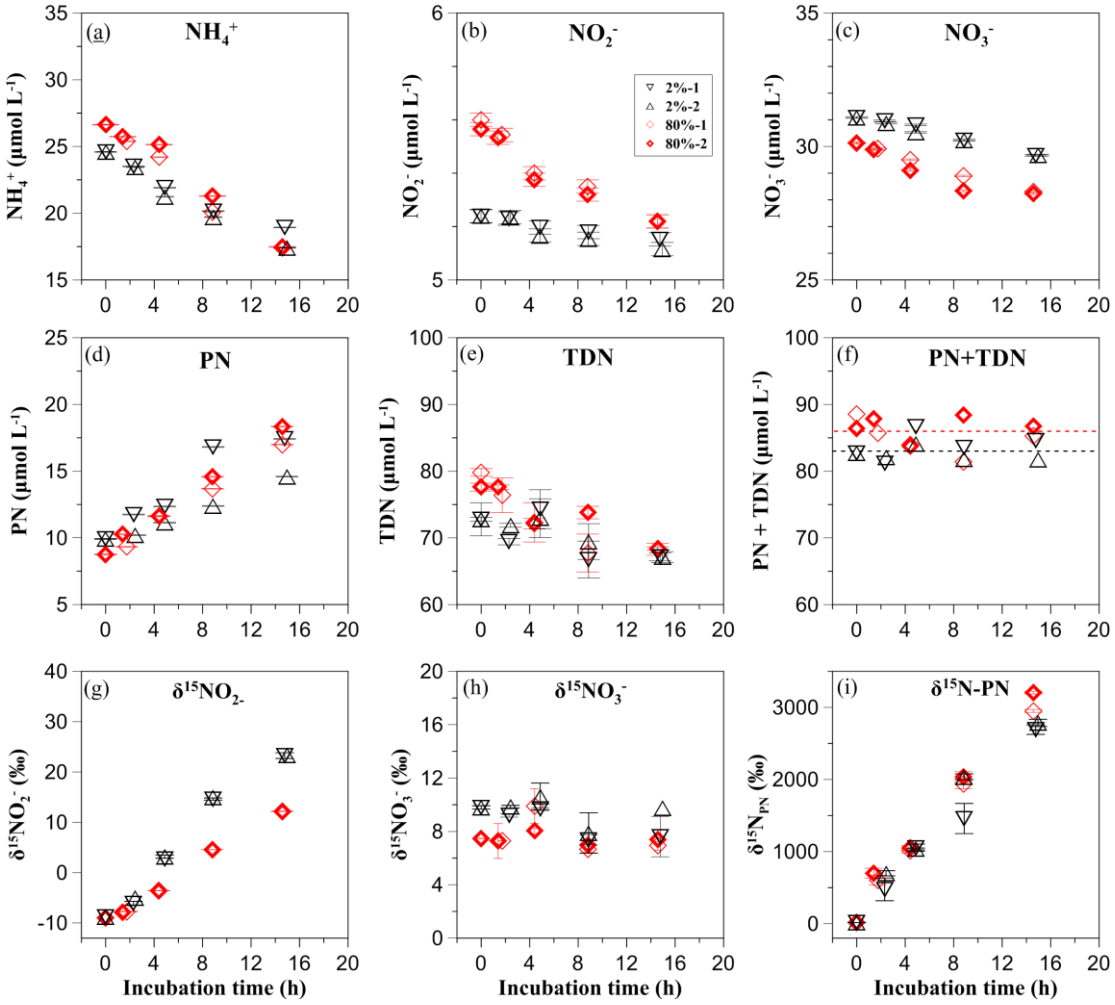

944

945

946 **Fig. 4**

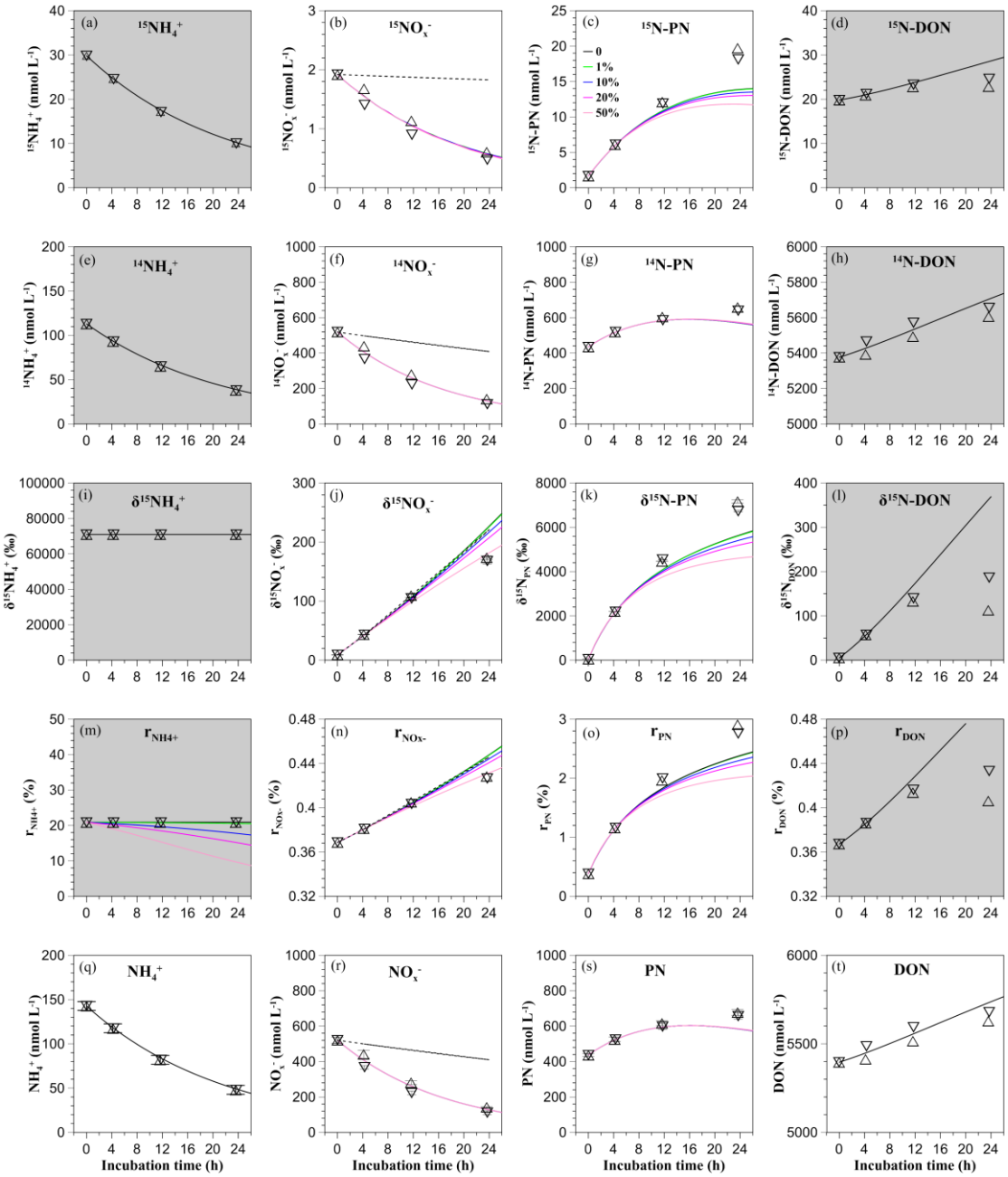

947

948

Fig. 5(A)

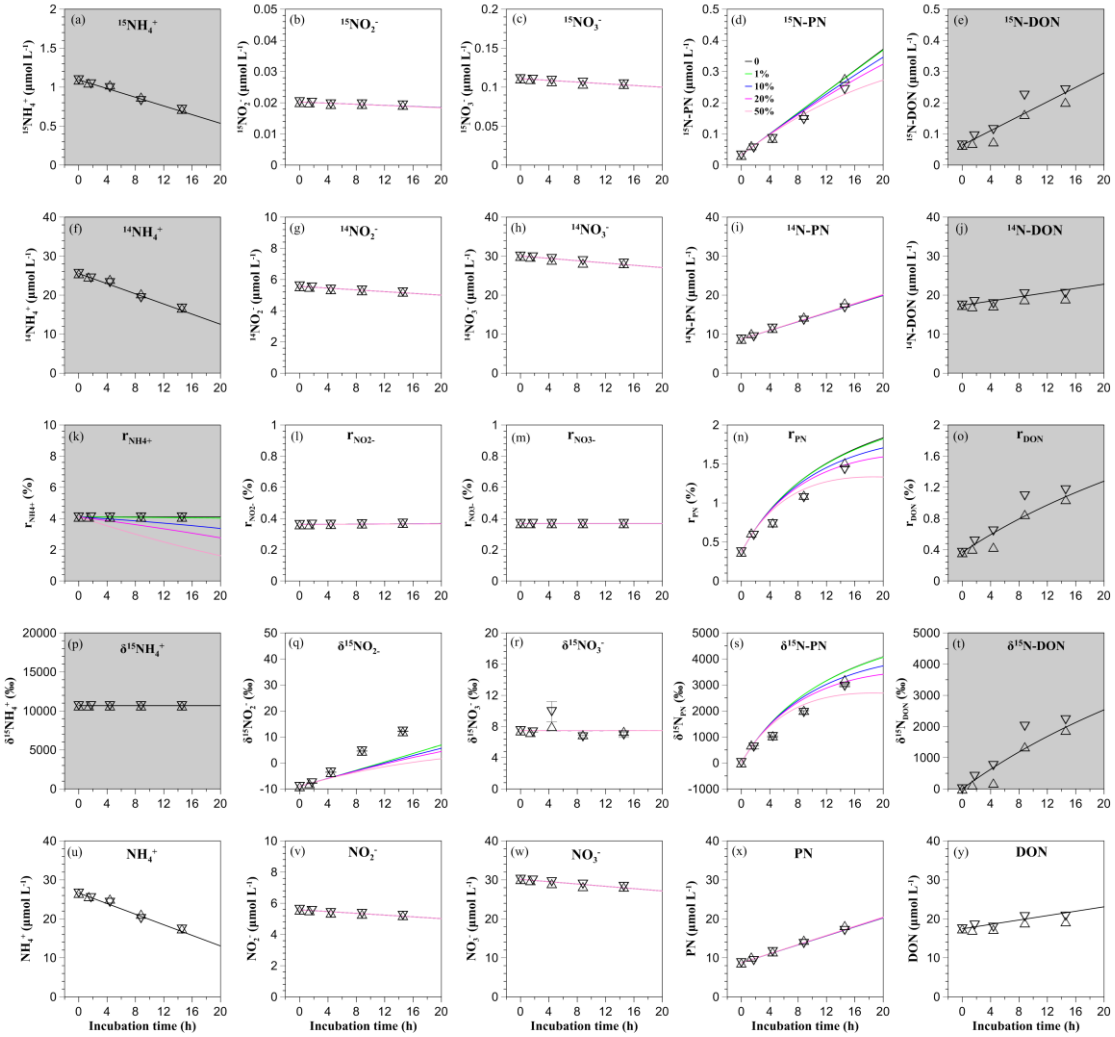
(a) $^{15}NH_4^+$
(b) $^{15}NO_2^-$
(c) $^{15}NO_3^-$
(d) ^{15}N-PN
(e) ^{15}N-DON
0
1%
10%
20%
50%
(f) $^{14}NH_4^+$
(g) $^{14}NO_2^-$
(h) $^{14}NO_3^-$
(i) ^{14}N-PN
(j) ^{14}N-DON
(k) r_{NH4+}
(l) r_{NO2-}
(m) r_{NO3-}
(n) r_{PN}
(o) r_{DON}
(p) $\delta^{15}NH_4^+$
(q) $\delta^{15}NO_2^-$
(r) $\delta^{15}NO_3^-$
(s) $\delta^{15}N$-PN
(t) $\delta^{15}N$-DON
(u) NH_4^+
(v) NO_2^-
(w) NO_3^-
(x) PN
(y) DON
Incubation time (h)

952 **Fig. 5(B)**

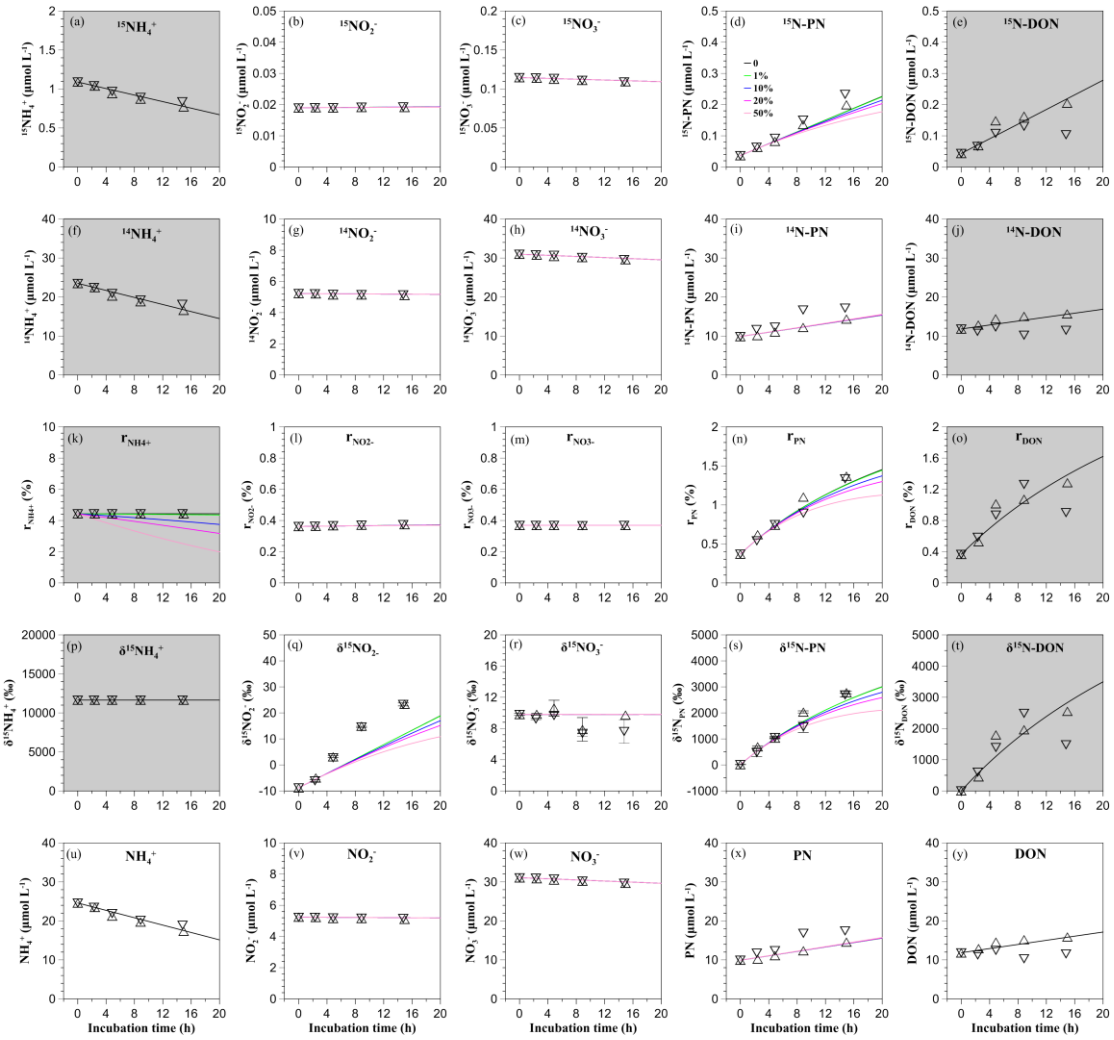

953